NASA CONTRACTOR REPORT

NASA CR-2479

NASA CR-2479

ISOLATED ROTOR NOISE DUE TO INLET DISTORTION OR TURBULENCE

by Ramani Mani

Prepared by
GENERAL ELECTRIC COMPANY
Schenectady, N.Y. 12301
for Lewis Research Center

NATIONAL AERONAUTICS AND SPACE ADMINISTRATION • WASHINGTON, D. C. • OCTOBER 1974

1. Report No.	2. Government Accession No.	3. Recipient's Catalog No.
NASA CR-2479		

4. Title and Subtitle	5. Report Date
ISOLATED ROTOR NOISE DUE TO INLET DISTORTION OR TURBULENCE	October 1974
	6. Performing Organization Code

7. Author(s)	8. Performing Organization Report No.
Ramani Mani	None
	10. Work Unit No.

9. Performing Organization Name and Address	11. Contract or Grant No.
General Electric Company P. O. Box 43 Schenectady, New York 12301	NAS 3-17853
	13. Type of Report and Period Covered
12. Sponsoring Agency Name and Address	Contractor Report
National Aeronautics and Space Administration Washington, D.C. 20546	14. Sponsoring Agency Code

15. Supplementary Notes

Final Report. Project Manager, James H. Dittmar, V/STOL and Noise Division, NASA Lewis Research Center, Cleveland, Ohio

16. Abstract

The report presents the theoretical formulation, analysis, and results necessary to analyze quadrupole noise generated from a loaded, isolated, subsonic rotor because of its interaction with an inflow distortion or inlet turbulence. The ratio of quadrupole to dipole noise is largely a function of the axial flow Mach number, wheel tip Mach number, rotor solidity, and total pressure ratio across the rotor. It is relatively independent of the specific form of the inflow distortion or inlet turbulence. Comparisons with experimental data only succeed in predicting gross levels at a given speed and fail to predict the variation of noise at fixed speed with flow and pressure ratio. Likely sources of this discrepancy are discussed.

17. Key Words (Suggested by Author(s))	18. Distribution Statement
Airplane engine noise Inlet distortion Inlet turbulence	Unclassified - unlimited

19. Security Classif. (of this report)	20. Security Classif. (of this page)	21. No. of Pages	22. Price*
Unclassified	Unclassified	43	$3.25

* For sale by the National Technical Information Service, Springfield, Virginia 22151

TABLE OF CONTENTS

SUMMARY

The present report presents the theoretical formulation, analysis and results necessary to analyze quadrupole noise generated from a loaded, isolated, subsonic rotor due to its interaction with an inflow distortion or inlet turbulence. Programs to calculate these interactions are given in an appendix. These programs also yield dipole noise contributions from these two mechanisms. The ratio of quadrupole to dipole noise is largely a function of the axial flow Mach number, wheel tip Mach number, rotor solidity, total pressure ratio across the rotor. It is relatively independent of the specific form of the inflow distortion or inlet turbulence. Comparisons with experimental data only succeed in predicting gross levels at a given speed and fail to predict the variation of noise at fixed speed with flow and pressure ratio. Looking at the separate variations of the theoretical predictions of dipole and quadrupole noise, however, one notices that if these levels were closer together, a suitable composite of them would yield the trends of the experimental data. This leads to a suggestion that the calculation may be overestimating the ratio of dipole to quadrupole noise by overestimating the dipole noise. Likely sources of this overestimate are suggested along with corrective procedures.

INTRODUCTION

The purpose of the present study is to quantify a quadrupole noise source which was first proposed in (2) as a likely contributor to fan noise. The source arises from the fluctuating Reynolds stresses introduced by a combination of two unsteady velocities, one being due to the potential flow field of the rotor and the other due to a solenoidal velocity field such as an inlet distortion or inlet turbulence.

The study proceeds as follows. Since interest is in fan/compressor noise where substantial duct axial velocities are involved, a pertinent Lighthill equation including uniform axial flow is derived first for the study of quadrupole noise. Secondly the potential flow fields of a subsonic rotor are derived as a function of the pressure ratio across it, the wheel tip and axial flow Mach numbers. Thirdly a systematic approach to the acoustic problem of estimating the noise from this source is worked out based on repeated use of Fourier exponential transforms.

We next present calculations under several constraints of the relative magnitudes of the quadrupole versus the dipole noise source. Comparisons are also carried out with some available data on the influence of pressure ratio on fan noise. In an appendix, computer programs for calculations of quadrupole and dipole noise due to both inlet distortion and inlet turbulence are given.

Ivan H. Edelfelt of the General Electric Research and Development Center helped considerably in programming these calculations. Thomas F. Gelder and Marvin E. Goldstein of the NASA-Lewis Research Center provided several helpful discussions.

DEVELOPMENT OF PERTINENT LIGHTHILL EQUATION FOR BLADE LOADING NOISE

The full Lighthill equation for aerodynamic noise for an inviscid gas, in the absence of mass, energy or force sources (and assuming the isentropic relation $p = a_o^2 \rho$) may be written as:

$$\frac{\partial^2 \rho}{\partial t^2} - a_o^2 \nabla^2 \rho = \frac{\partial^2}{\partial x_i \partial x_j} (\rho u_i u_j) \quad . \quad . \quad . \qquad (1)$$

Now let $u_i = U \delta_{1i} + u_i'$ where U is uniform and steady and 1 corresponds to the axial direction. Then we may show rigorously that (1) reduces to:

$$[\frac{\partial}{\partial t} + U \frac{\partial}{\partial x}]^2 \rho - a_o^2 \nabla^2 \rho = \frac{\partial^2}{\partial x_i \partial x_j} (\rho u_i' u_j') \quad . \quad . \quad . \qquad (2)$$

Equation (2) is the desired form of the Lighthill equation for blade loading noise from an isolated rotor. The form of $\rho u_i' u_j'$, correct to second order, would be $(\rho_o u_i' u_j')$. For an axial flow device, two important sources of velocity fluctuations are solenoidal velocity fluctuations associated with inlet distortion or inlet turbulence and secondly irrotational velocity fluctuations associated with the flow field of a loaded rotor. Thus we may write $u_i' = u_{is}' + u_{ip}'$ where u_{is}' denotes the solenoidal velocity fluctuation associated with inlet distortion or turbulence and u_p' that associated with the rotor potential flow field. The calculation of the quadrupole noise field due to interaction between the rotor potential flow field and an inlet distortion or turbulence field thus boils down to solving (2) with a source term of type,

$$2 \frac{\partial^2}{\partial x_i \partial x_j} (\rho_o u_{ip}' u_{js}').$$

The factor of 2 arises from the symmetry of the quadrupole term with respect to interchange of i, j.

DETERMINATION OF FLUCTUATING VELOCITIES DUE TO THE ROTOR POTENTIAL FLOW FIELD

For the determination of the fluctuating velocity field of the rotor, the most convenient quantity is the (nondimensional) lift coefficient of the steady lift exerted by the rotor blades on the fluid. However the quantities most conveniently available in practical terms are the pressure ratio across the rotor, its wheel tip and axial flow Mach numbers, etc. So we first evaluate C_L in terms of these quantities.

The work per lbm of the flow is

$$C_L \frac{\rho W_r^2 \, c \cos(\alpha_r) V}{2\rho U d} = \frac{\sigma C_L}{2} \frac{U^2 \sin(\alpha_r)}{\cos^2(\alpha_r)}$$

$$= C_p T_{01} (\frac{T_{02}}{T_{01}} - 1)$$

$$= \frac{\gamma\, RT_1(1 + \frac{\gamma - 1}{2} M_a^2)}{(\gamma - 1)} \{(\frac{p_{02}}{p_{01}})^{\frac{\gamma - 1}{\gamma}} - 1\}$$

$$\therefore \quad \frac{\sigma\, C_L \sin(\alpha_r)}{\cos^2(\alpha_r)\{\frac{2}{(\gamma - 1)M_a^2} + 1\}} = (\frac{p_{02}}{p_{01}})^{\frac{\gamma - 1}{\gamma}} - 1$$

This gives the desired expression for C_L as:

$$C_L = \frac{\cos^2(\alpha_r)}{\sigma \sin(\alpha_r)} \{1 + \frac{2}{(\gamma - 1)M_a^2}\}\{(\frac{p_{02}}{p_{01}})^{\frac{\gamma - 1}{\gamma}} - 1\}$$

To calculate the u', v' (x and y components of velocity) requires a linearized, compressible analysis of the flow field of the isolated rotor.

Let $W_r = a\, M_r$. We first find the solution for velocity components u', v', parallel to the x' - y' coordinate system of Figure 1, due to equally spaced concentrated unit forces at the origin and its corresponding points as shown in Figure 1. (Note that the blade exerts a force on the fluid equal and opposite to the force by the fluid on the blade.) We use a frame of reference fixed w.r.t. the translating blade row so that we have a steady state problem. We have to consider the effect of a sum of forces:

$$\underline{1} \sum_{n = -\infty}^{\infty} \delta(x')\, \delta[y' - 2n \frac{d}{2}]$$

where $\underline{1}$ denotes a unit force vector, and δ stands for the Dirac delta function. By using a result on page 68 of (1) concerning the sum of an infinite row of equally spaced delta functions, clearly the above is equal to:

$$\frac{1}{d}\, \delta(x') \sum_{n = -\infty}^{\infty} \exp[j \frac{2\pi n y'}{d}]$$

The linearized equations of motion and continuity are:

$$\rho[\frac{\partial u'}{\partial x'} + \frac{\partial v'}{\partial y'}] + W_r[\cos(\alpha_r)\frac{\partial \rho'}{\partial x'} + \sin(\alpha_r)\frac{\partial \rho'}{\partial y'} = 0 \qquad (1a)$$

$$\cos(\alpha_r)\frac{\partial u'}{\partial x'} + \sin(\alpha_r)\frac{\partial u'}{\partial y'} = -\frac{1}{\rho\, W_r}\, \frac{\partial p'}{\partial x'} + \frac{\sin(\alpha_r)\delta(x')}{\rho\, d\, W_r}$$

$$\sum_{-\infty}^{\infty} \exp(j \frac{2\pi n y'}{d})] \qquad (1b)$$

and

$$\cos(\alpha_r)\frac{\partial v'}{\partial x'} + \sin(\alpha_r)\frac{\partial v'}{\partial y'} = -\frac{1}{\rho W_r}\frac{\partial p'}{\partial y'}$$

$$\frac{-\cos(\alpha_r)\delta(x')}{\rho d W_r}\left[\sum_{-\infty}^{\infty} \exp\left(j\frac{2\pi n y'}{d}\right)\right] \qquad (1c)$$

Eliminating p' from (1b, c) we derive that:

$$\left[\cos(\alpha_r)\frac{\partial}{\partial x'} + \sin(\alpha_r)\frac{\partial}{\partial y'}\right]\left[\frac{\partial u'}{\partial y'} - \frac{\partial v'}{\partial x'}\right.$$

$$\left. - \frac{\delta(x')}{\rho W_r d}\sum_{-\infty}^{\infty} \exp\left(j\frac{2\pi n y'}{d}\right)\right] = 0$$

and since u', v' and the delta function term vanish far from the blade row

$$\frac{\partial u'}{\partial y'} - \frac{\partial v'}{\partial x'} = \frac{\delta(x')}{\rho W_r d}\sum_{-\infty}^{\infty} \exp\left[j\frac{2\pi n y'}{d}\right] \qquad (2)$$

[Kutta Joukowski Law]

Next we eliminate the force terms in (1b, c) and assuming an isentropic relation between p' and ρ' one obtains:

$$\frac{\partial u'}{\partial x'}\left[1 - M_r^2\cos^2(\alpha_r)\right] + \frac{\partial v'}{\partial y'}\left[1 - M_r^2\sin^2(\alpha_r)\right]$$

$$= M_r^2\sin(\alpha_r)\cos(\alpha_r)\left[\frac{\partial u'}{\partial y'} + \frac{\partial v'}{\partial x'}\right] \qquad (3)$$

(modified continuity equation)

Using (2), (3) single equations for u', v' may be obtained which may be solved by requiring that u', v' vanish as $x' \to \pm\infty$. We omit the details and give the result.

u' for $x' \gtrless 0$ =

$$-\frac{1}{2\rho d W_r}\frac{\left[\mathrm{sgn}(n)^*\, j\sqrt{1 - M_r^2} \pm M_r^2\sin(\alpha_r)\cos(\alpha_r)\right]}{(1 - M_r^2\cos^2\alpha_r)}$$

$$\sum_{-\infty}^{\infty} \exp\left(j\frac{2\,ny'}{d}\right)\exp\left[\frac{2\pi n x'\left[j\,M_r^2\sin(\alpha_r)\cos(\alpha_r) \mp \mathrm{sgn}(n)\sqrt{1 - M_r^2}\right]}{d(1 - M_r^2\cos^2(\alpha_r))}\right] \qquad (4a)$$

Similarly:

v' for $x' \gtrless 0$ =

$$\frac{\mp 1}{2\rho d W_r}\sum_{n=-\infty}^{\infty} \exp\left(j\frac{2\pi n y'}{d}\right)\exp\left(\frac{2\pi n x'}{d(1 - M_r^2\cos^2\alpha_r)}\right.$$

*sgn(n) = 1 if n > 0, = -1 if n < 0 and = 0 if n = 0.

$$[j\, M_r^2 \cos(\alpha_r)\sin(\alpha_r) \mp \mathrm{sgn}(n)\sqrt{1 - M_r^2}]) \qquad (4b)$$

When viewed in a frame of reference fixed with respect to the casing of the machine, these u', v' velocities given by (4a), (4b) appear as:

$$u' \text{ for } x \gtrless 0 = \frac{-C_L\ \sigma\ W_r}{4(1 - M_a^2)} \sum_{-\infty}^{\infty} \{\pm M_a\ M_t + \mathrm{sgn}(n) j\sqrt{1 - M_r^2}\}$$

$$\exp(j\,\frac{2\pi n y}{d})\exp[\frac{2\pi n x(\mp\ \mathrm{sgn}(n)\sqrt{1 - M_r^2} + j\ M_x\ M_t}{d(1 - M_x^2)}]$$

$$\exp(j\,\frac{2\pi n\ Vt}{d}) \ . \ . \ . \qquad (5a)$$

$$v' \text{ for } x \gtrless 0 =$$

$$\mp\,\frac{C_L\ \sigma\ W_r}{4} \sum_{-\infty}^{\infty} \exp(j\,\frac{2\pi n y}{d})\exp(\frac{2\pi n x(\mp\ \mathrm{sgn}(n)\sqrt{1 - M_r^2} + j\ M_x\ M_t}{d(1 - M_x^2)})$$

$$\exp(j\,\frac{2\pi n\ Vt}{d}) \qquad (5b)$$

THE AXIAL VELOCITY OF THE INLET DISTORTION

Far upstream from the rotor, the inlet distortion appears as regions of axial velocity defect superposed on a uniform inlet velocity.

Some assumption regarding the form of the inlet distortion is necessary in order to analyze its effect. The form assumed is sketched in Figure 2.

Let the axial velocity, in Mach number, associated with the uniform total pressure region be M_a. The axial velocity defect ΔM_a associated with the inlet distortion may be deduced as follows from the condition that far upstream there is no variation of static pressure.

$$\frac{p_t - \Delta p_t}{p} = \{1 + \frac{\gamma - 1}{2}(M_a - \Delta M_a)^2\}^{\frac{\gamma}{\gamma - 1}} \qquad (6)$$

(γ is the specific heat ratio of the gas)
Now

$$\frac{p_t}{p} = (1 + \frac{\gamma - 1}{2} M_a^2)^{\frac{\gamma}{\gamma - 1}} \qquad (7)$$

Thus one may solve for ΔM_a in (6) as:

$$\Delta M_a = M_a - \left[\frac{2}{\gamma - 1}\left\{\left(1 - \frac{\Delta p_t}{p_t}\right)^{\frac{\gamma - 1}{\gamma}} \left(1 + \frac{\gamma - 1}{2} M_a^2\right) - 1\right\}\right]^{1/2} \quad (8)$$

The form of Eq. (8) indicates that $\Delta p_t/p_t$ and M_a are subject to a restriction that

$$\left(1 - \frac{\Delta p_t}{p_t}\right)^{\frac{\gamma - 1}{\gamma}} \left(1 + \frac{\gamma - 1}{2} M_a^2\right) > 1 \quad (9)$$

(Other than the above restriction, M_a and $\Delta p_t/p_t$ may be specified arbitrarily.)

The restriction of (9) follows from the assumption that the distortion consists of regions of constant static pressure and varying axial velocity. For such a distortion, (9) simply expresses the requirement that the static pressure not exceed the total pressure anywhere. For small $\Delta p_t/p_t$, and small M_a^2, (9) may be expressed approximately as

$$\frac{\Delta p_t}{p_t} \leq \frac{\gamma}{2} M_a^2 \quad (9)$$

The interaction of the inlet distortion with the isolated rotor may be analyzed (as sketched in Figure 2) as the interaction of a shear wave, convecting along the fan inlet duct at an axial Mach number M_a, with an isolated rotor.

Let the inlet distortion be Fourier analyzed in an x-y coordinate system at the mean radius of analysis "a" as follows. The basic periodicity of the distortion in the y-direction is "2πa"/S (for an S lobed distortion). Let the distorted velocity profile be expressed as:

$$\sum_{i=-\infty}^{\infty} \exp(-j\, iS\, \frac{y}{a}) C_i \quad (10)$$

Here $j = \sqrt{-1}$, i = dummy index of summation.

$$C_i = \frac{-S}{2\pi a} \int_0^{\frac{2\pi a}{S}} \Delta M_a(y)\, e^{jiS\frac{y}{a}}\, dy \quad (11)$$

THEORY OF QUADRUPOLE NOISE GENERATION BY INLET DISTORTION

$$\text{Let } A = \frac{C_L\, \sigma\, W_r\, M_a\, M_t}{4(1 - M_a^2)}\,, \quad A' = 2A$$

$$B = \frac{C_L \sigma W_r \sqrt{1 - M_r^2}}{4(1 - M_a^2)}, \quad B' = 2B$$ (Sometimes B is also used to denote the number of rotor blades and the context of its use makes this fairly clear.)

$$C = \frac{+C_L \sigma W_r}{4}, \quad C' = 2C$$

$$\alpha_n = \frac{2\pi |n| \sqrt{1 - M_r^2}}{d(1 - M_a^2)} \qquad (-\infty < n < \infty)$$

$$\beta_n = \frac{2\pi n}{d} \qquad (-\infty < n < \infty)$$

$$\gamma_n = \beta_n M_t \qquad (-\infty < n < \infty)$$

$$\delta_n = \frac{2\pi n M_a M_t}{d(1 - M_a^2)} \qquad (-\infty < n < \infty)$$

$$\varepsilon_n = \beta_n S/nB \qquad (-\infty < n < \infty)$$

Only an axial quadrupole of type $\rho_o u_p u_s$ and a transverse one of type $\rho_o v_p u_s$ where u_p, v_p are the axial and tangential velocity distortions associated with the rotor potential flow field and u_s the axial velocity distortion associated with the inlet distortion contributes to the noise (at blade passing frequency and its multiples).

Exploiting the three facts that (a) there is no interest in the zeroth harmonic of blade passing frequency (which is a dc field) (b) that the rotor is subsonic ($M_r < 1$) and (c) we are only interested in propagating noise fields, we may show that the noise generation for a particular harmonic "n" (≥ 1) of blade passing frequency noise is governed by:

$$\left\{\frac{\partial}{a_o \partial t} + M_a \frac{\partial}{\partial x}\right\}^2 p - \nabla^2 p$$

$$= \frac{-\partial^2}{\partial x^2} \rho_o \left\{(\pm A' + j B') \sum_{i=1}^{\infty} C_i' \right.$$

$$\left. \exp(-\alpha_n |x|) \exp(j \delta_n x) \exp\left(j \beta_n \left(1 - \frac{is}{nB}\right) y\right)\right.$$

$$\mp \frac{\partial^2}{\partial x \partial y} \rho_o C' \sum_{i=1}^{\infty} C_i' \exp(-\alpha_n |x|) \exp(j \delta_n x) \exp\left(j \beta_n \left(1 - \frac{is}{nB}\right) y\right)$$

$$\exp[j\,\beta_n\,M_t\,a_o t]\}\ \ldots \qquad (1)$$

(where $C_i' = a_o\,C_i$)
Clearly p depends on y, t (given i) as

$$\exp[j\,\beta_n(1 - \tfrac{iS}{nB})y]\exp[j\,\beta_n\,M_t\,a_o t].$$

Thus we deduce that the axial part of p depends on x as:

$$\frac{d^2p}{dx^2}(1 - M_a^2) - 2j\,M_a\,M_t\,\beta_n(\frac{dp}{dx})$$

$$+ \beta_n^2\{M_t^2 - (1 - \tfrac{iS}{nB})^2\}p$$

$$= + \rho_o\,\frac{\partial^2}{\partial x^2}(\pm A' + j\,B')C_i'\exp(-\alpha_n|x|)\exp(j\,\delta_n\,x)$$

$$\pm \frac{\partial}{\partial x}\rho_o\,j\,C'\,\beta_n(1 - \tfrac{iS}{nB})\exp(-\alpha_n|x|)\exp(j\,\delta_n\,x) \qquad (2)$$

To solve (2) introduce the Fourier exponential transform P(z) of p by:

$$P(z) = \int_{-\infty}^{\infty} p\,e^{-jzx}\,dx$$

so that

$$p = \frac{1}{2\pi}\int_{-\infty}^{\infty} P(z)\,e^{jzx}\,dz$$

Then:

$$(z - z_+)(z - z_-)P(z)$$

$$= \frac{-2j\,z[A'(z - \delta_n)z - \alpha_n\,z\,B' + C'(z - \delta_n)\beta_n(1 - \tfrac{iS}{nB})]C_i'\,\rho_o}{[\alpha_n^2 + (z - \delta_n)^2](1 - M_a^2)} \qquad (3)$$

where

$$z_\pm = \frac{\beta_n}{(1 - M_a^2)}\{M_a\,M_t \mp \sqrt{M_t^2 - (1 - M_a^2)(1 - \tfrac{iS}{nB})^2}\}$$

Let

$$G(z) = \frac{-2j\,z\,C_i'\{A'(z - \delta_n)z - \alpha_n\,z\,B' + C'(z - \delta_n)\beta_n(1 - \tfrac{iS}{nB})\}\rho_o}{[\alpha_n^2 + (z - \delta_n)^2](1 - M_a^2)} \qquad (4)$$

By the method of residues, the downstream/upstream waves have amplitudes given by:

$$\frac{|G(z_\pm)|}{|z_+ - z_-|} = A_\pm \tag{5}$$

Independent waves (above cut-off) for each n will be produced over a range of i given by:

$$\frac{nB}{S}\left(1 - \frac{M_t}{\sqrt{1 - M_a^2}}\right) < i < \frac{nB}{S}\left(1 + \frac{M_t}{\sqrt{1 - M_a^2}}\right)$$

For each of these i, amplitudes of upstream and downstream waves are computed from (5). It is demonstrable that the rms values of the axial components of the intensity are (power/cross sectional area of annulus):

$$\frac{|A_\pm^2|\Delta M_t(1 - M_a^2)^2}{2\rho_o a_o(M_t \mp \Delta M_a)^2} \tag{6}$$

where

$$\Delta = [M_t^2 - (1 - M_a^2)(1 - \frac{iS}{nB})^2]^{1/2}.$$

This completes the theory of inlet distortion quadrupole noise generation.

NOISE GENERATION BY INLET TURBULENCE

We represent the turbulent velocity components by:

$$(u_t, v_t, w_t) = \int_{\text{all } \bar{k}} dZ_{u,v,w}(\bar{k}) e^{j(\bar{k}\cdot\bar{r})} e^{-jk_x Ut}$$

adopting the usual Fourier Stieltjes form where

$$\overline{dZ_u(\bar{k}')dZ_v(\bar{k}'')} = \delta(\bar{k}' - \bar{k}'')\Phi_{uv}(\bar{k}')d^3\bar{k}'\, d^3\bar{k}''$$

and $\Phi_{uv}(\bar{k})$ is the usual spectral density tensor.

The noise generation problem is given by:

$$\left[\frac{\partial}{a_o \partial t} + M_a \frac{\partial}{\partial x}\right]^2 p - \nabla^2 p = 2\rho_o\left\{\frac{\partial^2}{\partial x^2}(u_p u_t) + \frac{\partial^2}{\partial x \partial y}(u_p v_t + v_p u_t) + \frac{\partial^2}{\partial y^2}(v_p v_t)\right\}. \tag{7}$$

A typical term of the RHS of (7) may be written as:

$$-\rho_o \frac{\partial^2}{\partial x^2} \{(\pm A + \text{sgn}(n) j\, B) dZ_u(\ldots)\}$$

$$-\rho_o \frac{\partial^2}{\partial x\, \partial y} [(\pm A + j\, \text{sgn}(n) B) dZ_v(\ldots)$$

$$\pm C\, dZ_u(\ldots)] \mp \rho_o \frac{\partial^2}{\partial y^2} C\, dZ_v(\ldots) \tag{8}$$

where (...) stands for:

$$\exp[-\alpha_n |x|] \exp[j(\delta_n + k_x)x]$$

$$\exp[j(\beta_n + k_y)y] \exp[j[\beta_n M_t - M_a k_x] a_o t] \tag{9}$$

A word of explanation is in order here concerning the model of turbulence employed in the analysis. The model is the same as was employed in (3). A three dimensional model of turbulence is employed but the spectrum functions are integrated over the third coordinate (z) so that nowhere does the z dependence appear explicitly.

Substituting for the y dependence from (9), the source term (8) is effectively:

$$-\rho_o \frac{\partial^2}{\partial x^2} \{[\pm A + j\, \text{sgn}(n) B] dZ_u(\ldots)\}$$

$$-\rho_o \frac{\partial}{\partial x} j(\beta_n + k_y) \{(\pm A + j\, \text{sgn}(n) B) dZ_v \pm C\, dZ_u\}(\ldots)$$

$$\pm (\beta_n + k_y)^2 \rho_o C\, dZ_v(\ldots) \tag{10}$$

As before the Fourier exponential transform of the term in (10) may be written as:

$$\frac{-2j\, \rho_o}{\alpha_n^2 + [z - (\delta_n + k_x)]^2} \{z[z([z - (\delta_n + k_x)]A - \text{sgn}(n) B\, \alpha_n)$$

$$+ C(z - \delta_n - k_x)(\beta_n + k_y)] dZ_u$$

$$+ (\beta_n + k_y) \{z[(z - \delta_n - k_x)A - \alpha_n\, \text{sgn}(n) B]$$

$$+ (\beta_n + k_y)(z - \delta_n - k_x) C\} dZ_v\} \tag{11}$$

$$= \{G_u(z) dZ_u + G_v(z) dZ_v\} \tag{12}$$

where the definitions of $G_u(z)$ and $G_v(z)$ are obvious.

As before the downstream and upstream waves will have form:

(i) if $(\beta_n M_t - k_x M_a) > 0$, then with

$$z_{\pm} = \frac{1}{(1 - M_a^2)} \{(\beta_n M_t - k_x M_a)M_a$$

$$\mp [(\beta_n M_t - k_x M_a)^2 -$$

$$(1 - M_a^2)(\beta_n + k_y)^2]^{1/2}\}$$

the waves are given by

$$\frac{j[G_u(z_{\pm})dZ_u + G_v(z_{\pm})dZ_u]}{(1 - M_a^2)|z_+ - z_-|}$$

$$\exp[j z_{\pm} x]\exp[j(\beta_n + k_y)y]$$

$$\exp[j(\beta_n M_t - k_x M_a)a_o t] \qquad (13)$$

(ii) If $(\beta_n M_t - k_x M_a) < 0$, then

$$z_{\pm} = \frac{1}{(1 - M_a^2)} \{(\beta_n M_t - k_x M_a)M_a$$

$$\pm [(\beta_n M_t - k_x M_a)^2 -$$

$$(1 - M_a^2)(\beta_n + k_y)^2]^{1/2} \qquad (14)$$

and the rest is as in (13).

Let $\Delta = [(\beta_n M_t - k_x M_a)^2 - (1 - M_a^2)(\beta_n + k_y)^2]^{1/2}$ (15a)

and

$$f = |\beta_n M_t - k_x M_a| \qquad (15b)$$

Then the acoustic energy produced downstream and upstream by such waves is given by taking the mean square of (13) and multiplying the resulting quantity by:

$$\frac{1}{2\rho_o a_o} \{\frac{\Delta f(1 - M_a^2)^2}{(f \mp M_a \Delta)^2}\} \qquad (16)$$

The remaining procedure is more or less mechanical. Let us say that the interest is in the acoustic energy between wave numbers lying between χ and $\chi + \Delta\chi$. (Wave number = frequency in radians/sec. ÷ speed of sound). This determines that for each n from $-\infty$ to ∞, a range of k_x lying between:

$$[\beta_n \tan(\alpha_r) - \frac{\chi}{M_a}] \text{ to } \{\beta_n \tan \alpha_r - \frac{\chi}{M_a} - \frac{\Delta\chi}{M_a}\} \qquad (17)$$

is of interest. This determines (for each n) a specific value of k_x. A range of k_y from

$$\mp \frac{\chi}{\sqrt{1 - M_a^2}} - \beta_n \leq k_y \leq \pm \frac{\chi}{\sqrt{1 - M_a^2}} - \beta_n \qquad (18)$$

is to be considered (depending on whether χ is positive or negative). The quantity

$$G_u^2(z_\pm)\Phi_{uu} + 2G_u(z_\pm)G_v(z_\pm)\Phi_{uv} + G_v^2(z_\pm)\Phi_{vv}$$

times the factor in (16) is to be integrated over the range of k_y indicated in (18), given χ, β_n (and hence k_x by (17)) for each n in range $-\infty$ to ∞. For given physical wave number of interest both energy corresponding to $+\chi$ and $-\chi$ need to be considered. By adding up the infinite series of contributions from $n = -\infty$ to $n = \infty$ for $+\chi$ and $-\chi$, taking note of the fact that the width in k_x is $(\Delta\chi/M_a)$, etc., the required spectral density $dI^{\pm}/d\chi$ may be deduced. Φ_{uu}, Φ_{uv} and Φ_{vv} should first be integrated over k_z from $-\infty$ to ∞, in keeping with two dimensional or plane nature of present analysis. Actually it turns out to be more pertinent to think in terms of $\chi\, dI^{\pm}/d\chi$ as this quantity has the units of power and is related directly to measurements obtained by constant percent bandwidth or constant octave filters. If we assume a specific form of the longitudinal velocity correlation function for the turbulence of type $\exp(-r/L)$, Φ_{uu}, Φ_{uv} and Φ_{vv} can be easily written down for given turbulence intensity.

DISCUSSION OF RESULTS

Previously developed analyses (3, 4) of dipole noise were employed to estimate the dipole contribution to inlet distortion and inlet turbulence noise.

We show in Figures 3(a), (b), (c) first the nondimensional constant percent filter spectra due to inlet turbulence rotor interaction noise. We study a fixed operating line characterized by a steady lift coefficient of unity associated with a rotor whose solidity is unity. In turbulence noise calculations, one parameter that enters the calculation is the ratio of the integral length scale of turbulence to the blade spacing designated herein as (L/D). We have independently verified that the specific value of the ratio (L/D) does not materially affect the ratio of dipole/quadrupole noise contribution. For rotors with axial Mach numbers of order two-thirds the wheel tip Mach number, at wheel tip Mach numbers of order 0.8, the quadrupole noise contribution does indeed begin to exceed the dipole contribution especially at the higher frequencies. The low frequency end of the spectrum (frequencies less than half the blade passing frequency) is still dominated by dipole noise. Similarly calculations were carried out for a rotor with $(M_a/M_t) = 0.5$ and $C_L = 0.5$ and are shown in Figures 4(a), (b) and (c). Similar trends are evident insofar as the fact that the ratio of quadrupole/dipole contribution increases

with M_t and also, at a given M_t, increases with frequency. However one finds that the ratio of quadrupole/dipole noise, at given M_t, increases with the ratio (M_a/M_t). To bring this out in somewhat sharper focus, a calculation is shown in Figure 4(d) of a rotor with (M_a/M_t) being unity, at the same relative Mach number and lift coefficient, etc., as the rotor in Figure 4(c). The ratio of quadrupole/dipole noise is much greater in Figure 4(d) than in Figure 4(c). In Figures 5(a), (b), (c) and (d) are shown calculations of noise spectra at a fixed axial Mach number and total pressure ratio but with varying tip speed. Again as might be expected, higher tip speeds (and associated higher frequencies) do increase the relative ratio of quadrupole/dipole noise. However no evidence is available in these results to support the notion that fan noise could be minimized for constant work by choice of high tip speed and low loading. For other specific designs over some limited tip speed ranges, some such result may be true but it is certainly not a generally valid principle. Indeed the results of Figure 5 support the notion that for subsonic fans, to minimize noise for a given flow and total pressure ratio one should employ high blade loading and low tip speed. This conclusion applies of course only to the physical generation process and not to aspects such as effectiveness of treatment or perceived noise considerations.

In Figures 6 and 7, calculations corresponding to Figure 5 and Figure 3 are shown for 1st and 2nd harmonic pure tone (blade passing frequency) noise generated by an inlet distortion - rotor interaction. In both cases a maximum total pressure defect of 2% of the inlet total pressure was assumed. A four lobed distortion is assumed to impinge on a 38 bladed rotor. Other details are given in Figures 6, 7. A fairly smooth profile of the distortion as shown in Figures 6, 7 was assumed. The results of Figures 6, 7 are similar to those of Figures 5, 3 in that the ratio of quadrupole/dipole noise is greater for second harmonic rather than first harmonic noise and also increases with tip Mach number when a fixed operating line study is considered (ratio of (M_a/M_t) fixed, fixed C_L).

Finally an attempt was made to compare the results of the current analysis with experimental data from (5). The data given in (5) pertains to 50 Hz bandwidth forward radiated power at the blade passing frequency measured at several speeds and several pressure ratios at each speed. The data for two rotors (designated rotor 1 and rotor 2 in (5)) were employed.

Figure 8 indicates the results for rotor 1. This case has also been analyzed by the authors of (6) and, as assumed by them, a four lobed distortion with maximum velocity defect equal to 1% of the axial velocity is assumed to impinge on the rotor. The shape of the distortion was assumed to be a triangular pulse of width 10% of the extent of the lobe. This width corresponds roughly to the width of each of four struts placed upstream of the rotor in the experiments reported in (6).

Shown in Figure 8 are the actual measured data at 50, 60, 70 and 80% speeds and predictions by the current analysis using the results of the current study and those of (4). The dipole and quadrupole contributions are shown separately (as predicted by the theory). The dipole noise levels predicted by the theory are roughly in the ballpark of the results observed in (5) by Gelder and Soltis but in one major respect the theory fails completely. The present calculations employ the two dimensional Sears gust formula for estimation of unsteady forces needed to obtain the dipole noise. According to these results, the dipole noise greatly

exceeds the quadrupole noise (by at least 10 dB) over the operating range of rotor 1 of (5). Since dipole noise is independent of blade loading and is proportional to the rotor relative velocity (which decreasea as the loading is raised at constant wheel tip speed), the inlet noise is always predicted to decrease with increasing pressure ratio (and associated lower weight flow and rotor relative velocities). The data of (5) of course fail to show this trend at all.

In case of rotor 2, an attempt was made to predict the noise (in a 50 Hz bandwidth) with the aid of the turbulence noise prediction procedures. Measurements of scale and intensity of turbulence are pretty scarce but a good set of measurements for one flow condition and one inlet is available in (9) and these were crudely scaled to the conditions of the inlet in (5). A 4% intensity of turbulence effective over the outer 10% of the rotor blade span and an (L/D) of about 0.5 was assumed for these calculations. Again one notices a fair ability to account for the gross noise levels by the inlet turbulence dipole noise theoretical estimates but a total failure to predict the variation with pressure ratio and flow at fixed speed largely due to the extreme predominance of dipole noise according to the theoretical estimates.

To put these results in perspective, we start by remarking that the quadrupole noise mechanism pointed out in (2) is a second order effect while dipole noise is a first order effect. Thus, with a dipole mechanism, the acoustic pressures scale roughly as $(\rho_o W_r u')$ where ρ_o = mean fluid density, W_r = steady relative velocity through the rotor and u' the fluctuating solenoidal velocity (whether due to distortion or turbulence). With a quadrupole noise mechanism, they scale as $(\rho_o u_p u')$ where u_p is the potential flow field induced by the rotor and generally $u_p << W_r$. Indeed the very procedure adopted to estimate u_p is a small perturbation calculation assuming that u_p and $v_p << W_r$.

Again the full quadrupole source term $\frac{\partial^2}{\partial x_i \partial x_j}(\rho_o u_i u_j)$ may be expanded as $(\theta^2 + 2u_i \frac{\partial \theta}{\partial x_i} + (\frac{\partial u_j}{\partial x_i})(\frac{\partial u_i}{\partial x_j}))$ where θ is the divergence of the velocity. So far as the inflow distortion or inflow turbulence is concerned, these velocity fields have zero divergence. Even the potential flow field of the rotor does not have a significant divergence at modest axial and wheel tip Mach numbers. For $M_a = M_t$, for example, the divergence of the rotor velocity field is $M_a^2(\theta + 2(\partial u/\partial y))$ and thus of second order in the axial Mach number. Hence only the term $\rho_o(\frac{\partial u_j}{\partial x_i})(\frac{\partial u_i}{\partial x_j})$ of $\frac{\partial^2}{\partial x_i \partial x_j}(\rho_o u_i u_j)$ may be expected to contribute significantly. Finally the quadrupole source is an extended source subject to extensive phase cancellation while the dipole source is generally assumed to be compact (as is the case in the present model). In this regard it is interesting to note that the authors of (6) considered only the potential flow field upstream of the rotor plane as contributing to the upstream noise and it is possible that such an approach will involve less phase cancellation.

Rao and Chu (8) concur with the results of the current calculations in obtaining estimates of the ratio of dipole/quadrupole noise of the order of 20 dB. Morfey (7) has calculated noise from the axial quadrupole $(\rho_o u_p u_s)$ but it is difficult to see why he did not include the contribution of the x-y quadrupole $(\rho_o v_p u_s)$. Thus the term that Morfey calculates is

$\rho_o \frac{\partial^2}{\partial x^2}(u_p\, u_s)$. Actually if one includes the term $\frac{\partial^2}{\partial x\, \partial y}(\rho_o\, v_p\, u_s)$ the quadrupole noise source term can be written as

$$\rho_o \frac{\partial u_s}{\partial y}\frac{\partial v_p}{\partial x} + \rho_o\, u_s \frac{\partial \theta_p}{\partial x}$$

where θ_p = divergence of rotor potential flow field = $(\frac{\partial u_p}{\partial x} + \frac{\partial v_p}{\partial y})$. For the low Mach number applications considered by Morfey (he has $0 \leq M_t \leq M_a$ and $M_a < 0.7$) and especially for the Mach numbers ($M_a \sim 0.25$) where he claims the quadrupole mechanism overtakes the dipole mechanism, θ_p was probably negligible and thus the term he should have dealt with was really $\rho_o \frac{\partial u_s}{\partial x}\frac{\partial v_p}{\partial x}$. The term that he really employed viz. $\rho_o \frac{\partial^2}{\partial x^2}(u_p\, u_s)$ is actually more or less cancelled by a part of $\frac{\partial^2}{\partial x\, \partial y}(\rho_o\, v_p\, u_s)$. Thus a serious question arises with regard to the correctness of his relative estimates of the quadrupole/dipole mechanism.

We are still left however with the question of the total failure of the present results in Figures 8, 9 to agree with the data of (5). Two remarks are in order here. First of all, absolute prediction is really much less of a goal than the prediction of relative trends. This is because absolute prediction requires a whole host of good inputs other than the acoustic data such as distortion, turbulence data which have only been estimated in this case. Paradoxically of course the present predictions have done somewhat better on absolute prediction than on the relative trends. We notice consistently from Figures 8, 9 that if the dipole-quadrupole levels were more closely matched, the relative trends in the data would be much better explained. In other words, the actual data in Figures 8, 9 often exhibit trends intermediate between those of the dipole and quadrupole noise trends considered separately. Needless to say, since the dipole noise is predicted to be so much higher than the quadrupole source, any attempt to simply add them algebraically would of course fail to explain the data trends. This brings us to the second remark. It appears that the present calculations may be considerably overestimating the ratio of dipole/quadrupole energy. The quadrupole noise calculation is, in many respects, the more exact calculation. The dipole noise estimate employs the Sears gust formula and there are indeed several reasons for believing that it leads to overestimation of the unsteady force. Note that the Sears gust formula applies only to plane, incompressible flows involving isolated, flat plate airfoils at zero angle of attack. Firstly accounting for longitudinal or chordwise gusts generally leads to reduced values of gust loads (7). For inlet distortion noise, the reduction may be estimated as $(\tan(\alpha_r) - C_L/\pi)/\tan(\alpha_r)$. Secondly suggestions have been made that the Sears function could be revised to accommodate real fluid effects by multiplying it by the steady value of $(dC_L/d\alpha)$ at finite loading to the steady value of $(dC_L/d\alpha)$ at zero loading. This correction would have to be determined experimentally but $(dC_L/d\alpha)$ generally decreases with increasing loading (or C_L) becoming zero before the airfoil stalls. Similarly inclusion of finite aspect ratio effects or of gust obliquity would also lead to

lowered estimates of unsteady loads (see (6) for suggestions on including the aspect ratio effect - the suggested procedure is very similar to the one concerning real fluid effects). Finally compressibility and cascade effects also generally tend to lower estimates of the gust loads. The work of Timman (10) on compressibility effects at high Mach numbers for isolated airfoils does predict a reduced gust load (at fixed reduced frequency). The source compactness assumed in the present calculations for dipole noise may again be a source of overestimation in view of the tendency of phase cancellation to occur with a distributed source.

One final remark with regard to Morfey's study (7) is that by choice of a distortion with period equal to the blade spacing (one that is not likely to occur in practice), he starts, a priori, with a situation of low gust loads due to the very high reduced frequencies involved. Also he considered a rotor of unusually low tip solidity = 0.5, a model which again inherently favors the quadrupole mechanism.

CONCLUSIONS

1. A systematic theory of quadrupole noise generation in fans/compressors has been worked out both for inlet distortion and inlet turbulence - rotor noise. The calculations along with previously developed analyses of dipole noise due to these agencies have been coded into working programs included in the present report.

2. Parametric calculations with hypothetical constraints indicate that:

   a) At any fixed operating point, the ratio quadrupole/dipole noise increases with frequency whether one considers inlet turbulence or inlet distortion to be the source of noise.

   b) Along a fixed operating line, i.e. for fixed (M_a/M_t) and for given C_L, the ratio of quadrupole to dipole noise increases with tip Mach number.

   c) At fixed M_a and given total pressure ratio, the variation of ratio of quadrupole to dipole noise with tip Mach number is not very simple. This is because with increasing tip speed and fixed pressure ratio, the loading (or C_L) decreases with tip speed but the frequencies increase. These features are illustrated in Figure 5 where the ratio of quadrupole to dipole noise is minimum in Figure 5(c) at $M_t = .6$.

   d) The ratio of quadrupole/dipole noise is largely a function of M_a, M_t, rotor solidity and pressure ratio (or C_L) and largely independent of the specific form of the distortion or turbulence (within broad limits).

   e) The analysis shows the quadrupole noise to be independent of rotor solidity (at fixed M_a, M_t and total pressure ratio) but dipole noise increases with rotor solidity and hence the ratio of quadrupole to dipole noise decreases with increasing rotor solidity.

3. No general support is obtained for the idea that for given total pressure ratio, fan noise can be lowered by operating at high tip speed and low loading based on present calculations (see Figure 5).

4. Comparisons with data from two rotors as reported in (5) reveal that the analysis does fairly well in predicting the gross PWL levels at given speeds but fails substantially in predicting the trends of the variation of PWL at fixed speed with flow and pressure ratio. When this deficiency is examined in detail, it is found that if one looks at the separate theoretical predictions of the trends of variation of PWL due to dipole and quadrupole mechanisms, the data of (5) often exhibit trends intermediate to those of the dipole and quadrupole predictions. However, the theory consistently places the dipole noise levels at values much higher than the quadrupole levels for the design parameters of the two rotors studied in (5) and hence a composite of the two theoretical predictions does not exhibit the trend of the real data of (5) at all. A possible inference from this is that the ratio of dipole/quadrupole noise is overestimated by the theory and it is argued that this may be chiefly due to overestimate of the gust loads by relying on the Sears gust formula to predict them. Modifications to the gust formula to allow for real fluid, chordwise gust, aspect ratio, spanwise variation, compressibility and cascade effects are all suggested refinements likely to bring the predicted levels of dipole and quadrupole noise much closer together. If this happens, it is possible that a composite of the two will result in predicted trends in much better agreement with the data of (5).

APPENDIX 1

COMPUTER PROGRAMS FOR CALCULATION OF DIPOLE AND QUADRUPOLE NOISE DUE TO INLET DISTORTION OR TURBULENCE

INLET DISTORTION NOISE

Inputs needed are:

TPD	total pressure defect, maximum value of $(\Delta p_t)/p_t$.
IS	number of lobes in distortion.
EMA	M_a
EMT	M_t
NDP	number of points used to specify the distortion shape (see Figure A1), should be less than 51.
GAM	γ
RHØ	gas density in lbm/cft.
C	speed of sound in fps.
A	area of annulus being studied in square feet.
N	harmonic of blade passing noise of interest.
IB	number of rotor blades.
SIGR	σ
TPR	(p_{02}/p_{01})
TPDS(I)	NDP values specifying relative shape of total pressure distortion (max. value would be unity: $0 \leq$ TPDS(I) ≤ 1). See Figure A1.

Outputs given are:

1) All inputs except NDP, TPDS(I).

2) Sound power in dB re: 10^{-13} watts in each lobe number M where M = N • IB - I • (IS). M, I are also printed. The dipole and quadrupole noise upstream and downstream are given as PUDDB, PDDDB, PUQDB, PDQDB. The sum over all propagating M is given as

SPUDDB	(dipole noise upstream),
SPDDDB	(dipole noise downstream),
SPUQDB	(quadrupole noise upstream) and
SPDQDB	(quadrupole noise downstream).

APPENDIX 1

INLET DISTORTION NOISE

Inputs needed are:

TPD	total pressure defect, maximum value of $(\Delta p_t)/p_t$.
IS	number of lobes in distortion.
EMA	M_a
EMT	M_t
NDP	number of points used to specify the distortion shape (see Figure A1), should be less than 51.
GAM	γ
RHØ	gas density in lbm/cft.
C	speed of sound in fps.
A	area of annulus being studied in square feet.
N	harmonic of blade passing noise of interest.
IB	number of rotor blades.
SIGR	σ
TPR	(p_{02}/p_{01})
TPDS(I)	NDP values specifying relative shape of total pressure distortion (max. value would be unity: $0 \leq$ TPDS(I) ≤ 1). See Figure A1.

Outputs given are:

1) All inputs except NDP, TPDS(I).

2) Sound power in dB re: 10^{-13} watts in each lobe number M where M = N · IB - I·(IS). M, I are also printed. The dipole and quadrupole noise upstream and downstream are given as PUDDB, PDDDB, PUQDB, PDQDB. The sum over all propagating M is given as

   SPUDDB (dipole noise upstream),
   SPDDDB (dipole noise downstream),
   SPUQDB (quadrupole noise upstream) and
   SPDQDB (quadrupole noise downstream).

INLET TURBULENCE NOISE

Inputs needed are:

EMA	M_a
EMT	M_t
TPR	(p_{02}/p_{01})
NELMAX	number of (L/D) needed to be investigated.
M	number of frequencies at which $f \frac{dI_{\pm}}{df}$ is desired.
TI	turbulence intensity $\langle u'^2 \rangle \div U^2$
GAM	γ
RHØ	ρ in lbm/cft.
CS	speed of sound in fps.
AI	cross sectional area of annulus of interest, sq. ft.
SIGR	σ

F(I)(I = 1, M): M values of frequency expressed as (f/f_b) where f_b = blade passing frequency.

ELIN(I)(I = 1, NELMAX): NELMAX values of (L/D) of interest.

Outputs are:

1) All inputs except NELMAX.

2) For each L/D (written as EL) and F, $10 \log_{10}[f \frac{dI_{\pm}}{df} \div \frac{5}{2} \rho U\langle u'\rangle^2]$ for both dipole and quadrupole sources as SDVDBR, SDDDBR, SQVDBR, SQDDBR. Also sum of dipole and quadrupole contributions to $[f \frac{dI}{df}]$, upstream and downstream re: 10^{-13} watts as PVDB and PDDB.

```
09999 FILENAME ØUTPUT
10000 DIMENSIØN AEV(46),AED(46),ZMM(46),ZPP(46),DCV1(91),DCD1(91),
10001 &          F(20),DCV2(91),DCD2(91),STHØSR(91),AEVETC(2,91),
10002 &          AEDETC(2,91),ELIN(25)
10010 ØUTPUT="ITØUT"
10020 BEGIN FILE ØUTPUT
10030 END FILE ØUTPUT
10100 100 FØRMAT(V)
10200 READ ("ITINPUT",100) LN,EMA,EMT,TPR
10205 READ ("ITINPUT",100) LN,NELMAX,M,TI
10210 READ ("ITINPUT",100) LN,GAM,RHØ,CS,AI,SIGR
10220 IBEG=1
10230 IEND=10
10240 240 IF (IEND .GT. M) IEND=M
10250 READ ("ITINPUT",100) LN,(F(I),I=IBEG,IEND)
10260 IF (IEND .EQ. M) GØ TØ 300
10270 IBEG=IBEG+10
10280 IEND=IEND+10
10290 GØ TØ 240
10300 300 IBEG=1
10310 IEND=10
10320 320 IF (IEND .GT. NELMAX) IEND=NELMAX
10330 READ ("ITINPUT",100) LN,(ELIN(I),I=IBEG,IEND)
10340 IF (IEND .EQ. NELMAX) GØ TØ 500
10350 IBEG=IBEG+10
10360 IEND=IEND+10
10370 GØ TØ 320
10500 500 WRITE (ØUTPUT,510)
10510 510 FØRMAT(//32H      EMA       EMT       M       TI)
10520 WRITE (ØUTPUT,530) EMA,EMT,M,TI
10530 530 FØRMAT(2F9.3,I6,F9.2)
10535 C=CS
10536 A=AI
10540 WRITE (ØUTPUT,550)
10550 550 FØRMAT(//53H      GAM       RHØ         C          A       SIGR
10551 &       TPR)
10560 WRITE (ØUTPUT,570) GAM,RHØ,C,A,SIGR,TPR
10570 570 FØRMAT(F9.3,F9.4,F9.0,F9.2,F8.2,F9.2)
10600 DBL=130.+4.342945*ALØG(.105*RHØ*(C*EMA)**3*TI**2*A)
10610 PI=3.1415926
10615 TPI=2.*PI
10620 G1ØV2=(GAM-1.)/2.
10630 G1ØVG=(GAM-1.)/GAM
10640 EMR=SQRT(EMA**2+EMT**2)
10650 T11=TPR**G1ØVG-1.
10660 T12=1.+1./(G1ØV2*EMA**2)
10670 SR1MM2=SQRT(1.-EMA**2)
10680 SR1MR2=SQRT(1.-EMR**2)
10690 CR=EMA/EMR
10695 CR2=CR*CR
10700 SR=EMT/EMR
10705 SR2=SR*SR
10710 SRCR=SR*CR
```

```
10715 TR=EMT/EMA
10720 EMRC=EMR/(5.*CR)
10730 CL=CR2*T12*T11/(SIGR*SR)
10740 AA=1.-EMA**2
10750 A=CL*SIGR*EMA*EMT/(4.*AA)
10760 B=CL*SIGR*SRIMR2/(4.*AA)
10770 C=CL*SIGR/4.
10780 ALC=TPI*SRIMR2
10790 BETC=TPI
10800 CHIC=BETC*EMT
10810 DELC=TPI*EMA*EMT
10840 CDP=PI*SIGR/2.
10845 CDP2=CDP*CDP
10850 CAE=1./(EMA*SRIMM2)
10900 NINC02=10
10910 NINC=2*NINC02
10920 FNINC=NINC
10930 DELTH=PI/FNINC
10940 THETA=-PI/2.
10950 IMAX=NINC+1
11000 D0 1230 I=1,IMAX
11010 CTH=C0S(THETA)
11020 EMAMC=EMA-CTH
11030 EMAPC=EMA+CTH
11040 IF (I .GT. (NINC02+1)) G0 T0 1090
11050 ZMM(I)=EMAMC
11060 ZPP(I)=EMAPC
11070 AEV(I)=CAE/(1.+EMA*CTH)**2
11080 AED(I)=CAE/(1.-EMA*CTH)**2
11090 1090 STH=SIN(THETA)
11100 TERM=SRIMM2*STH*CR
11110 DCV1(I)=(EMAPC*SR-TERM)**2
11120 DCV2(I)=(EMAPC*SR+TERM)**2
11130 DCD1(I)=(EMAMC*SR-TERM)**2
11140 DCD2(I)=(EMAMC*SR+TERM)**2
11150 STH0SR(I)=STH/SRIMM2
11160 INDEX=I
11170 IF (I .GT. (NINC02+1)) INDEX=IMAX+1-I
11180 AEVETC(1,I)=AEV(INDEX)*CDP2*DCV1(I)
11190 AEVETC(2,I)=AEV(INDEX)*CDP2*DCV2(I)
11200 AEDETC(1,I)=AED(INDEX)*CDP2*DCD1(I)
11210 AEDETC(2,I)=AED(INDEX)*CDP2*DCD2(I)
11220 THETA=THETA+DELTH
11230 1230 C0NTINUE
11250 D0 3010 NEL=1,NELMAX
11255 EL=ELIN(NEL)
11260 WRITE (0UTPUT,1261) EL
11261 1261 F0RMAT(//11H  ***** EL=1P1E12.3,6H *****)
11270 CPHI=1./(4.*PI*EL)
11275 ELC=1./(EL*EL)
11300 D0 3000 J=1,M
11310 WRITE (0UTPUT,1320) F(J)
11320 1320 F0RMAT(//7H  F(J)=E12.3)
```

```
11330 CHI=F(J)*CHIC
11335 CHI2=CHI*CHI
11340 SDV=0.
11350 SDD=0.
11360 SQV=0.
11370 SQD=0.
11380 NVAL=8
11390 NVALP1=NVAL+1
11500 DØ 2800 NN=1,NVALP1
11510 N=NN-1
11520 IF (N) 1530,1550,1570
11530 1530 SGN=-1.
11540 GØ TØ 1580
11550 1550 SGN=0.
11560 GØ TØ 1580
11570 1570 SGN=1.
11580 1580 EN=N
11590 AL=ABS(EN)*ALC
11595 AL2=AL*AL
11600 ALSGNB=AL*SGN*B
11605 BET=EN*BETC
11610 DEL=DELC*EN
11630 SUMDV=0.
11640 SUMDD=0.
11650 SUMQV=0.
11660 SUMQD=0.
11670 THETA=-PI/2.
11800 DØ 2600 I=1,IMAX
11805 AKX=BET*TR-CHI/EMA
11810 AKY=-BET+CHI*STHØSR(I)
11820 AKY2=AKY*AKY
11830 INDEX=I
11840 IF (I .GT. (NINCØ2+1)) INDEX=IMAX+1-I
11850 ZM=ZMM(INDEX)*CHI
11860 ZP=ZPP(INDEX)*CHI
11900 DØ 2310 L1=1,2
11910 AKX2=AKX*AKX
11920 ELAKX2=ELC+AKX2
11930 CPHI1=CPHI/(ELAKX2+AKY2)**2.5
11940 PHIXX=(4.*AKY2+ELAKX2)*CPHI1
11950 PHIXY=-3.*AKY*AKX*CPHI1
11960 PHIYY=(4.*AKX2+ELC+AKY2)*CPHI1
11965 TPHIXY=2.*PHIXY
11970 ØMR=SIGR*(AKX*CR+AKY*SR)/2.
11980 SRF=1./(1.+TPI*ABS(ØMR))
11990 PHIT=PHIXX*SR2-TPHIXY*SRCR+PHIYY*CR2
11995 PHITS=PHIT*SRF
12000 IF (L1 .EQ. 2) GØ TØ 2040
12010 FNDVP=AEVETC(1,I)*PHITS
12020 FNDDP=AEDETC(1,I)*PHITS
12030 GØ TØ 2060
12040 2040 FNDVM=AEVETC(2,I)*PHITS
12050 FNDDM=AEDETC(2,I)*PHITS
```

```
12060 2060 ZTERM=ZP
12070 AKXA=AKX*AA
12080 DØ 2200 L2=1,2
12090 ZDELAK=ZTERM-DEL-AKXA
12100 DEN=(AL2+ZDELAK**2)**2
12110 PART=ZTERM*(ZDELAK*A-ALSGNB)+C*ZDELAK*CHI*STHØSR(I)*AA
12120 GX=ZTERM*PART
12130 GY=CHI*STHØSR(I)*PART*AA
12140 TQ=(GX**2*PHIXX+GY**2*PHIYY+GX*GY*TPHIXY)/DEN
12150 IF (L2 .EQ. 2) GØ TØ 2180
12160 FNQV=TQ*AEV(INDEX)
12170 GØ TØ 2190
12180 2180 FNQD=TQ*AED(INDEX)
12190 2190 ZTERM=ZM
12200 2200 CØNTINUE
12210 IF (L1 .EQ. 2) GØ TØ 2250
12220 FNQVP=FNQV
12230 FNQDP=FNQD
12232 AKX=BET*TR+CHI/EMA
12234 ZP=-ZP
12236 ZM=-ZM
12240 GØ TØ 2310
12250 2250 FNQVM=FNQV
12260 FNQDM=FNQD
12310 2310 CØNTINUE
12400 FDV=FNDVP+FNDVM
12410 FDD=FNDDP+FNDDM
12420 FQV=FNQVP+FNQVM
12430 FQD=FNQDP+FNQDM
12440 IF ((I .NE. 1) .AND. (I .NE. IMAX)) GØ TØ 2490
12450 FDV=FDV/2.
12460 FDD=FDD/2.
12470 FQV=FQV/2.
12480 FQD=FQD/2.
12490 2490 SUMDV=SUMDV+FDV
12500 SUMDD=SUMDD+FDD
12510 SUMQV=SUMQV+FQV
12520 SUMQD=SUMQD+FQD
12530 THETA=THETA+DELTH
12600 2600 CØNTINUE
12610 SNDV=CHI2*SUMDV*DELTH
12620 SNDD=CHI2*SUMDD*DELTH
12630 SNQV=SUMQV*DELTH
12640 SNQD=SUMQD*DELTH
12650 IF (N .GT. 0) GØ TØ 2750
12700 SDV=SDV+SNDV
12710 SDD=SDD+SNDD
12720 SQV=SQV+SNQV
12730 SQD=SQD+SNQD
12740 GØ TØ 2800
12750 2750 SDV=SDV+2.*SNDV
12760 SDD=SDD+2.*SNDD
12770 SQV=SQV+2.*SNQV
```

```
12780 SQD=SQD+2.*SNQD
12800 2800 CONTINUE
12802 SDV=SDV*EMRC
12803 SDD=SDD*EMRC
12804 SQV=SQV*EMRC
12805 SQD=SQD*EMRC
12810 SDVDBR=4.342945*ALOG(SDV)
12820 SDDDBR=4.342945*ALOG(SDD)
12830 SQVDBR=4.342945*ALOG(SQV)
12840 SQDDBR=4.342945*ALOG(SQD)
12850 PV=SDV+SQV
12860 PD=SDD+SQD
12870 PVDB=4.342945*ALOG(PV)+DBL
12880 PDDB=4.342945*ALOG(PD)+DBL
12900 WRITE (OUTPUT,2910)
12910 2910 FORMAT(//40H     SDVDBR     SDDDBR     SQVDBR     SQDDBR)
12920 WRITE (OUTPUT,2930) SDVDBR,SDDDBR,SQVDBR,SQDDBR
12930 2930 FORMAT(4F10.1)
12940 WRITE (OUTPUT,2950)
12950 2950 FORMAT(//20H       PVDB       PDDB)
12960 WRITE (OUTPUT,2970) PVDB,PDDB
12970 2970 FORMAT(2F10.1)
13000 3000 CONTINUE
13010 3010 CONTINUE
13100 STOP
13110 END
```

```
09990 FILENAME ØUTPUT
10000 DIMENSIØN SIGN(2),ETA(2),TPDS(50),DELM(500),PD(2),PQ(2)
10010 ØUTPUT="IDØUT"
10020 BEGIN FILE ØUTPUT
10030 END FILE ØUTPUT
10100 100 FØRMAT (V)
10200 READ ("IDINPUT",100) LN,TPD,IS,EMA,EMT,NDP
10210 READ ("IDINPUT",100) LN,GAM,RHØ,C,A,N,IB,SIGR,TPR
10220 IBEG=2
10230 IEND=11
10240 240 IF (IEND .GT. (NDP+1)) IEND=NDP+1
10250 READ ("IDINPUT",100) LN,(TPDS(I),I=IBEG,IEND)
10260 IF (IEND .EQ.(NDP+1)) GØ TØ 500
10270 IBEG=IBEG+10
10280 IEND=IEND+10
10290 GØ TØ 240
10500 500 S=IS
10510 EN=N
10520 B=IB
10600 WRITE (ØUTPUT,610)
10610 610 FØRMAT(///36H       TPD       IS        EMA         EMT)
10620 WRITE (ØUTPUT,630) TPD,IS,EMA,EMT
10630 630 FØRMAT(F10.3,I7,2F10.3)
10640 WRITE (ØUTPUT,650)
10650 650 FØRMAT(//65H      GAM       RHØ          C          A        N     IB
10651 &     SIGR       TPR)
10660 WRITE (ØUTPUT,665) GAM,RHØ,C,A,N,IB,SIGR,TPR
10665 665 FØRMAT(F9.3,F9.4,F9.0,F9.2,2I6,F9.3,F9.2)
10670 PI=3.1415926
10675 IMAX=500
10676 IMAX1=IMAX-1
10677 FIMAX1=IMAX1
10680 JMAX=NDP+2
10685 JMAX1=JMAX-1
10686 FJMAX1=JMAX1
10687 TPDS(1)=0.
10688 TPDS(JMAX)=0.
10690 DELM(1)=0.
10700 DELM(IMAX)=0.
10710 G1ØV2=(GAM-1.)/2.
10720 G1ØVG=(GAM-1.)/GAM
10730 T1=1.+G1ØV2*EMA**2
10740 T11=TPR**G1ØVG-1.
10750 T12=1.+1./(G1ØV2*EMA**2)
10760 DØ 800 I=2,IMAX1
10762 FI=I
10764 TERMI=(FI-1.)/FIMAX1
10766 J1=TERMI*FJMAX1+1.
10768 J2=J1+1
10770 FJ1=J1
10772 FJ2=J2
10774 TERMJ1=(FJ1-1.)/FJMAX1
10776 TERMJ2=(FJ2-1.)/FJMAX1
```

```
10778 TPDI=TPDS(J1)+(TPDS(J2)-TPDS(J1))*(TERMI-TERMJ1)/(TERMJ2-TERMJ1)
10780 TPDD=TPD*TPDI
10785 T2=(1.-TPDD)**G10VG
10790 DELM(I)=EMA-SQRT((T1*T2-1.)/G10V2)
10800 800 CONTINUE
10810 EMR=SQPT(EMA**2+EMT**2)
10820 SR1MM2=SQRT(1.-EMA**2)
10830 SR1MR2=SQRT(1.-EMR**2)
10840 IMIN=(1.-EMT/SR1MM2)*EN*B/S+.999
10850 IMAX=(1.+EMT/SR1MM2)*EN*B/S
10860 ALSRR=ATAN(EMT/EMA)
10870 VR=C*EMA/COS(ALSRR)
10880 CONST=(VR*VR*SIGR/2.)**2*A*RH0*746./(C*32.2*550.)
10890 SR=SIN(ALSRR)
10900 CXI=SR
10910 TXI=-COS(ALSRR)/SR
10920 CLT=COS(ALSRR)**2*T12*T11/(SIGR*SR)
10930 AA=1.-EMA**2
10940 AP=CLT*EMA*EMT/AA
10950 BP=CLT*SR1MR2/AA
10955 CP=CLT
10960 BB=EN*B*EMT
10970 BB2=BB*BB
10980 CC=EMA*BB
10990 DD=EMA/BB
11000 ALPH=EN*B*SR1MR2/AA
11010 SPUD=0.
11020 SPDD=0.
11030 SPUQ=0.
11040 SPDQ=0.
11050 SIGN(1)=1.
11060 SIGN(2)=-1.
11070 COM=PI*SR*SIGR*S/B
11080 CCLC=PI*SIN(2.*ALSRR)/EMA
11090 WRITE (OUTPUT,1800)
11100 DO 1900 I=IMIN,IMAX
11110 FI=I
11120 M=N*IB-I*IS
11130 EM=M
11200 DELTH=2.*PI/(S*FIMAX1)
11230 THETA=DELTH
11240 SUM1=0.
11250 SUM2=0.
11300 DO 400 K=2,IMAX1
11310 TERM=FI*S*THETA
11320 F1=DELM(K)*COS(TERM)
11330 F2=DELM(K)*SIN(TERM)
11340 SUM1=SUM1+F1
11350 SUM2=SUM2+F2
11360 THETA=THETA+DELTH
11400 400 CONTINUE
11410 TERM1=DELTH*S/(2.*PI)
11420 CIR=TERM1*SUM1
```

```
11430 CII=TERM1*SUM2
11440 CI=SQRT(CIR**2+CII**2)
11450 DEL=SQRT(BB2-AA*EM**2)
11460 TØPD=(CXI/DEL)*CCLC*CI
11470 EMTXI=EM*TXI
11480 TØPQ=CI/((ALPH**2+(DEL/AA)**2)*EMR)
11490 ØM=FI*CØM
11500 APP=.1811
11510 SEARS=SQRT((APP+ØM)/(APP+(PI*APP+1.)*ØM+2.*PI*ØM*ØM))
11600 DØ 1700 K=1,2
11610 CAY=(SIGN(K)*CC+DEL)/AA
11620 AØVFD=TØPD*CAY*(1.+EMTXI*SIGN(K)/CAY)*SEARS
11630 FI=CAY/SQRT(CAY**2+EM**2)
11640 F2=1.+SIGN(K)*CAY*DD
11650 ETA(K)=.5*(FI-SIGN(K)*EMA)/F2
11660 AØVFQ=CAY*(AP*DEL*CAY/AA-ALPH*BP*CAY*SIGN(K)+CP*SIGN(K)*DEL*
11661 & EM/AA)*TØPQ/DEL
11670 PD(K)=ETA(K)*AØVFD**2
11680 PQ(K)=ETA(K)*AØVFQ**2
11700 1700 CØNTINUE
11710 PUD=PD(1)*CØNST
11720 PDD=PD(2)*CØNST
11730 PUQ=PQ(1)*CØNST
11740 PDQ=PQ(2)*CØNST
11750 PUDDB=130.+4.342945*ALØG(PUD)
11760 PDDDB=130.+4.342945*ALØG(PDD)
11770 PUQDB=130.+4.342945*ALØG(PUQ)
11780 PDQDB=130.+4.342945*ALØG(PDQ)
11800 1800 FØRMAT (//50H     I     M       PUDDB       PDDDB       PUQDB
11801 &       PDQDB)
11810 WRITE (ØUTPUT,1820) I,M,PUDDB,PDDDB,PUQDB,PDQDB
11820 1820 FØRMAT (2I5,4F10.1)
11830 SPUD=SPUD+PUD
11840 SPDD=SPDD+PDD
11850 SPUQ=SPUQ+PUQ
11860 SPDQ=SPDQ+PDQ
11900 1900 CØNTINUE
11910 SPUDDB=130.+4.342945*ALØG(SPUD)
11920 SPDDDB=130.+4.342945*ALØG(SPDD)
11930 SPUQDB=130.+4.342945*ALØG(SPUQ)
11940 SPDQDB=130.+4.342945*ALØG(SPDQ)
11950 WRITE (ØUTPUT,1960)
11960 1960 FØRMAT (/41H      SPUDDB     SPDDDB     SPUQDB     SPDQDB)
11970 WRITE (ØUTPUT,1980) SPUDDB,SPDDDB,SPUQDB,SPDQDB
11980 1980 FØRMAT (4F10.1)
20000 STØP
20010 END
```

APPENDIX 2

LIST OF SYMBOLS

a_o, a	speed of sound.
a	sometimes used to denote radius of fan annulus being studied.
B	number of blades in the rotor.
C_L	lift coefficient of the rotor.
C	rotor chord.
C_p	specific heat at constant pressure.
C_i	coefficients of inlet distortion.
d	pitch of rotor.
j	$\sqrt{-1}$
L/D	integral length scale of turbulence/rotor pitch.
M_a, M_r and M_t	axial, relative and wheel tip Mach numbers.
p	pressure.
p_{02}/p_{01}	pressure ratio across rotor
p_t	local total pressure
R	gas constant
S	number of lobes in distortion.
T_{01}, T_{02}, T_1	total temperature upstream and downstream of rotor, temperature ahead of rotor.
U	axial velocity entering rotor.
V	wheel velocity.
W_r	relative velocity through rotor.
α_r	stagger angle of rotor.
δ_{ij}	Kronecker delta.
δ	delta function.
ρ	density.
σ	rotor solidity.

REFERENCES

1. J. E. Ffowcs Williams and D. L. Hawkings, "Theory Relating to the Noise of Rotating Machinery," Journal of Sound and Vibration, Vol. 10, 1969, p. 10.

2. Lighthill, M. J., Fourier Analysis and Generalized Functions, Cambridge University Press, 1962.

3. R. Mani, "Noise Due to Interaction of Inlet Turbulence with Isolated Stators and Rotors," Journal of Sound and Vibration, Vol. 17, No. 2, July-August 1971, pp. 251-260.

4. R. Mani, Simplified Procedure of Estimating Inlet Distortion -- Rotor Noise, General Electric Company Report No. 69-C-264, July 1969.

5. T. F. Gelder and R. F. Soltis, Inlet Plenum Chamber Noise Measurement Comparison of 20-Inch-Diameter Fan Rotors with Aspect Ratios 3.6 and 6.6, National Aeronautics and Space Administration TM X-2191, 1971.

6. M. Goldstein, J. Dittmar and T. Gelder, A Combined Quadrupole-Dipole Model for Inlet Flow Distortion Noise from a Subsonic Fan, National Aeronautics and Space Administration TN D-7676, 1974.

7. C. L. Morfey, "Tone Radiation from an Isolated Subsonic Rotor," The Journal of the Acoustical Society of America, Vol. 49, No. 5 (Part 2) (1971), pp. 1690-1692.

8. G. V. R. Rao and W. T. Chu, "Noise from an Isolated Rotor Due to Inflow Turbulence," British Acoustical Society: Spring Meeting at Chelsea College, London, April 25-27, 1973, paper No. 73ANC2.

9. J. A. Asher, M. Kurosaka, and S. D. Savkar, "Research on Noise Generation from Large Fan Engines," General Electric Research and Development Center Technical Report prepared for National Aeronautics and Space Administration Headquarters, July 1972, report No. SRD-72-079 (Rev.).

10. R. Timman, et al., "Aerodynamic Coefficients on an Oscillating Airfoil in Two-Dimensional Subsonic Flow," Journal of the Aeronautical Sciences, Vol. 18, No. 12, December 1951.

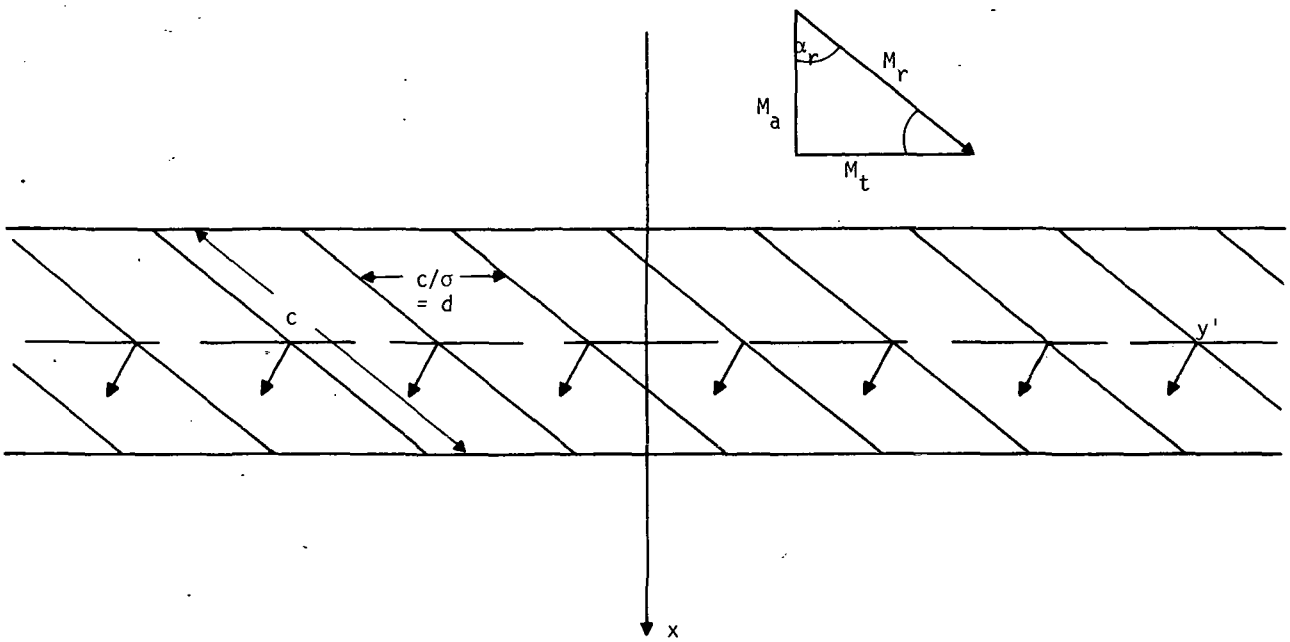

FIGURE 1

CALCULATION OF ROTOR POTENTIAL FLOW FIELD

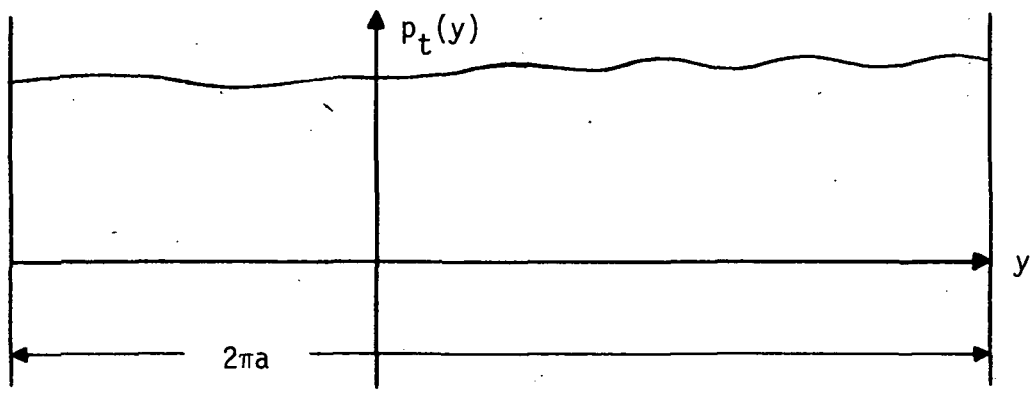

a = mean radius of annulus

FIGURE 2

VARIATION OF TOTAL PRESSURE AROUND THE ANNULUS

FIGURE 3. INLET TURBULENCE - ROTOR NOISE

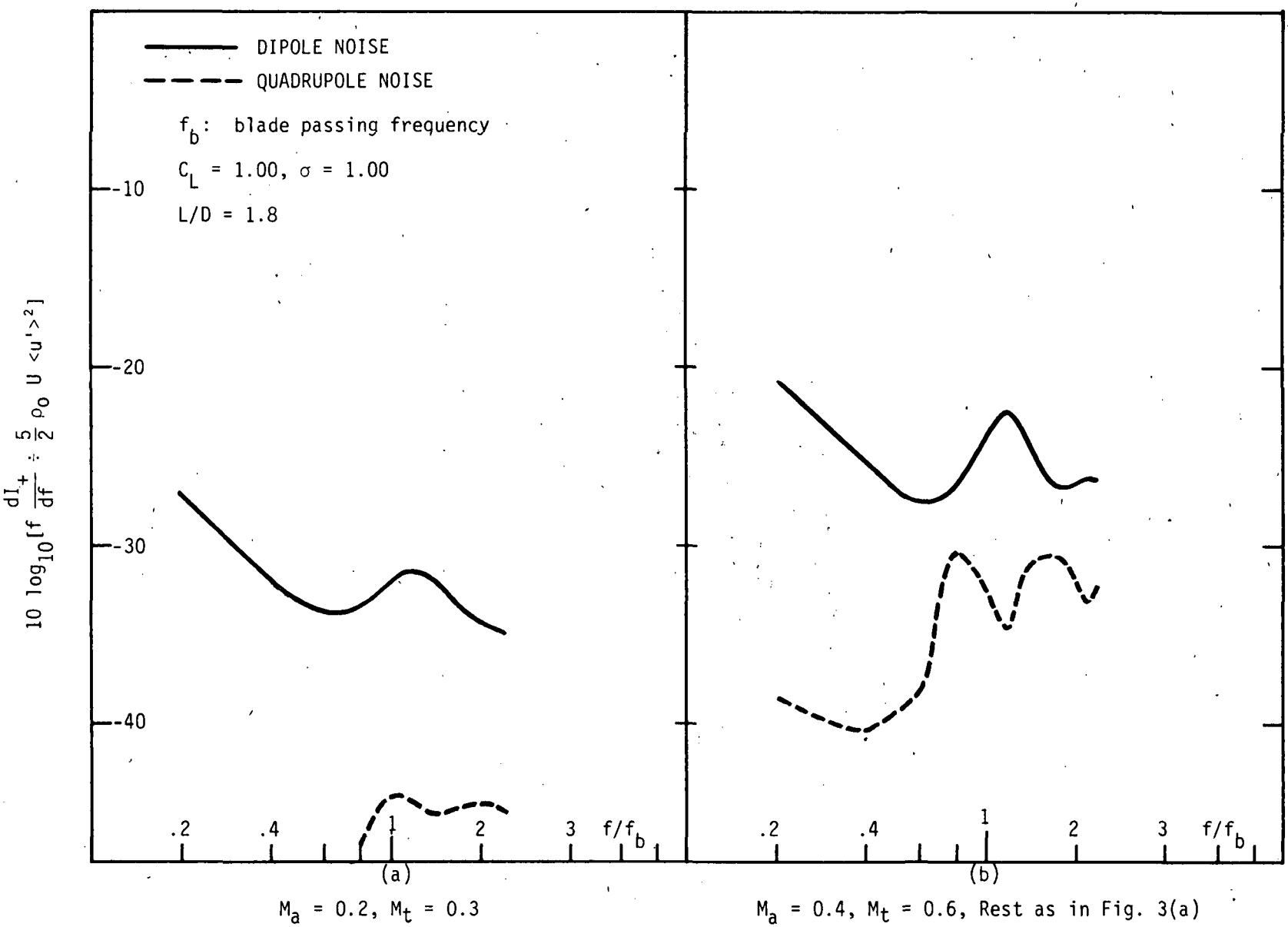

M_a = 0.2, M_t = 0.3

M_a = 0.4, M_t = 0.6, Rest as in Fig. 3(a)

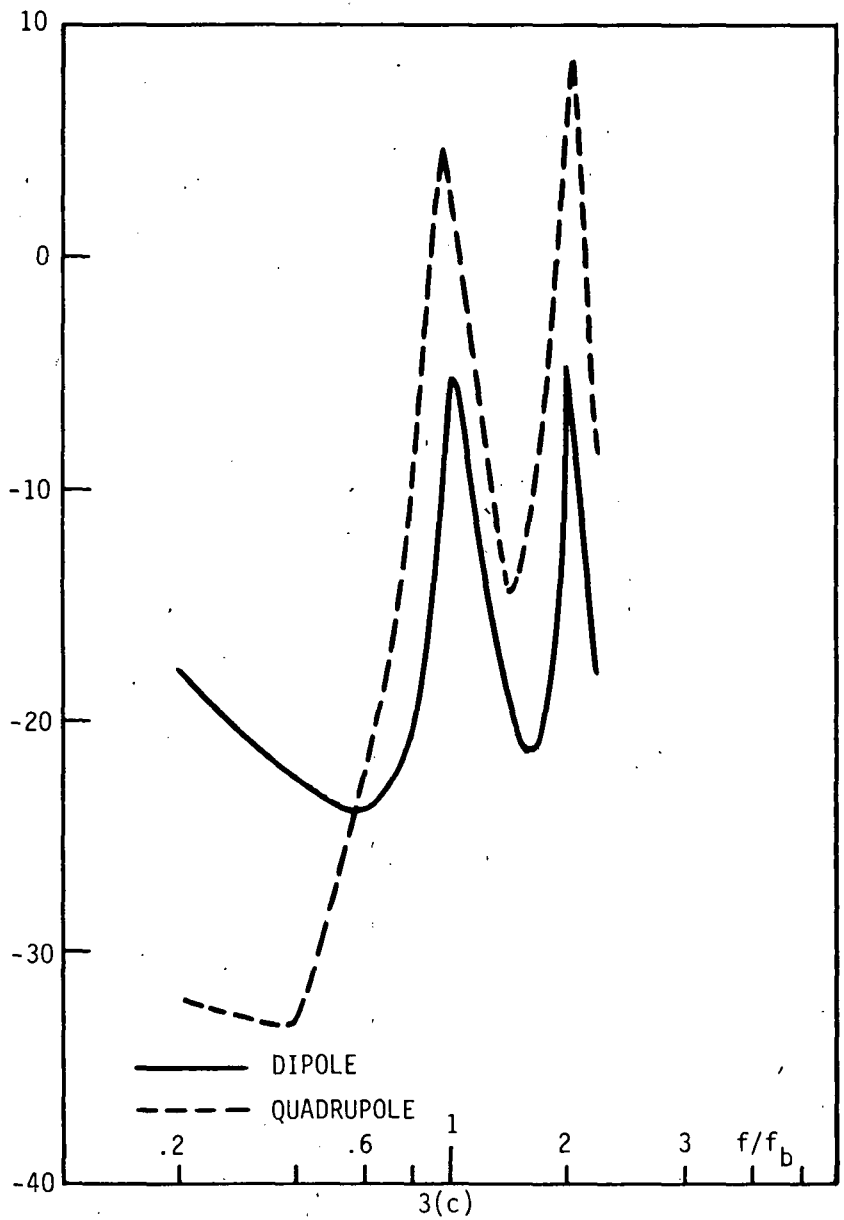

M_a = 0.55, M_t = 0.825, Rest as in Figure 3(a)

FIGURE 4. INLET TURBULENCE - ROTOR NOISE (Contd.)

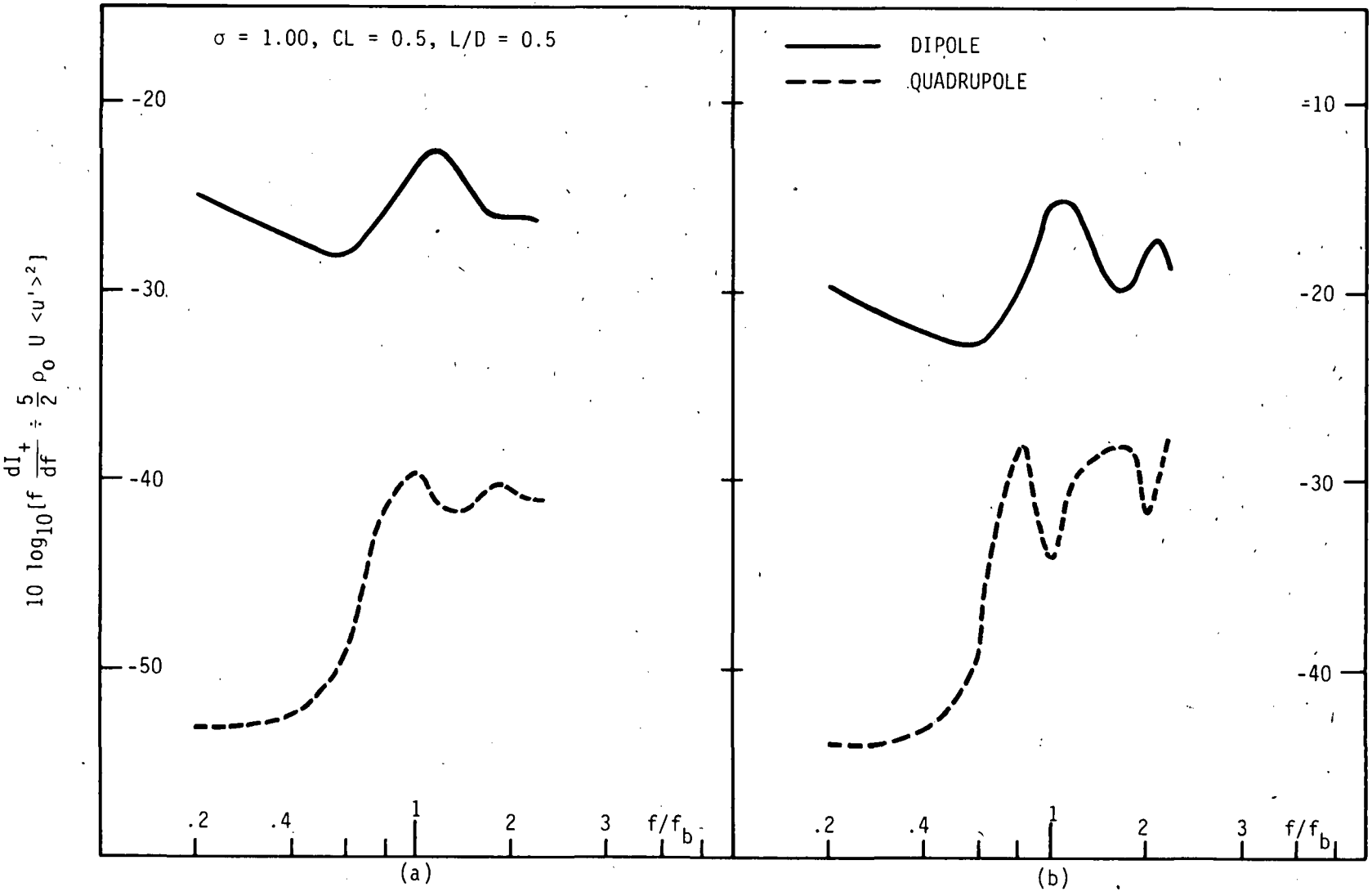

M_a = 0.2, M_t = 0.4

M_a = 0.35, M_t = 0.7, Rest as in 4(a)

FIGURE 4 (Concluded)

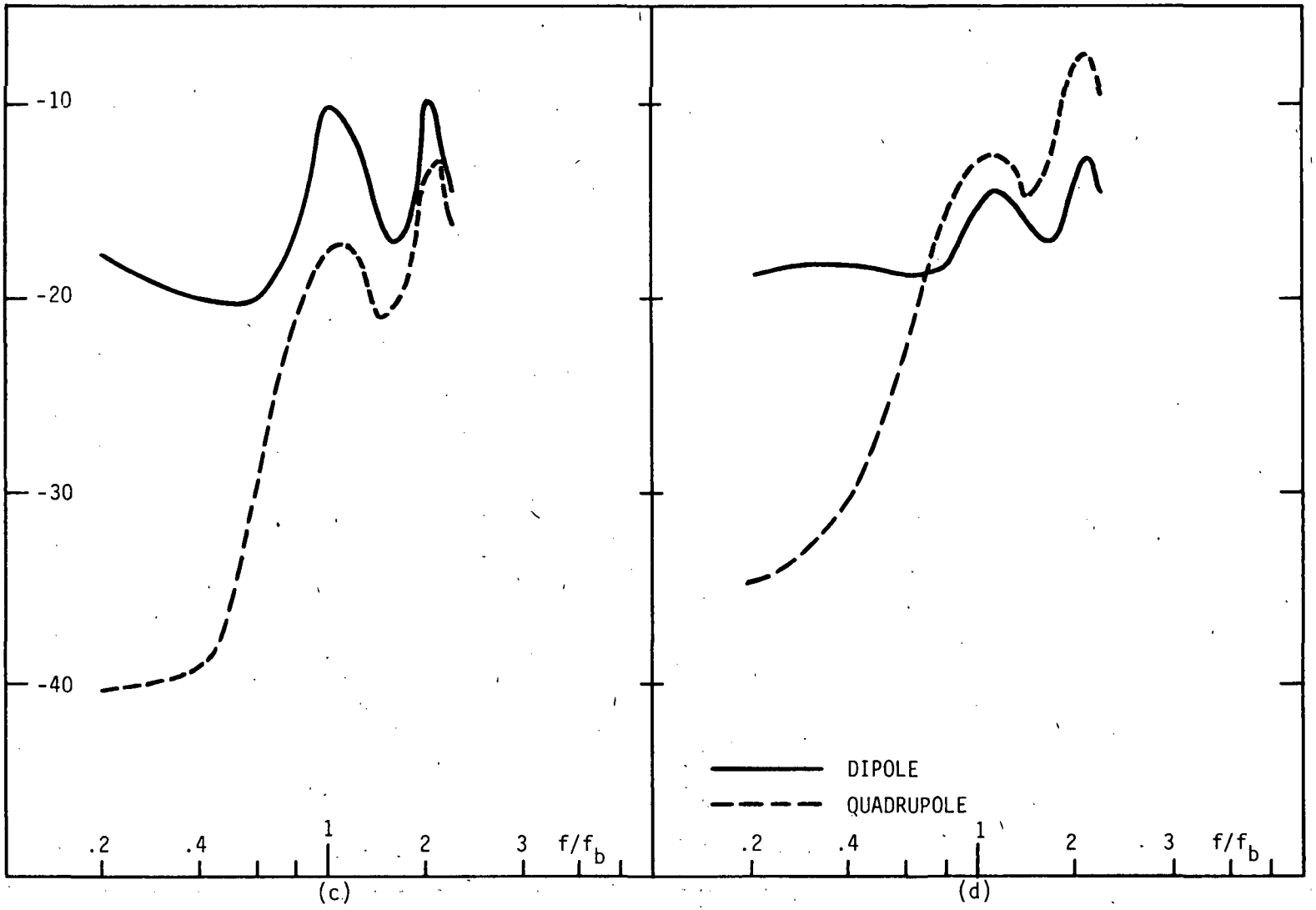

M_a = .425, M_t = .85, Rest as in 4(a)

M_a = 0.7, M_t = 0.7, Rest as in 4(a)

FIGURE 5. EFFECT OF TIP SPEED AT CONSTANT PRESSURE RATIO

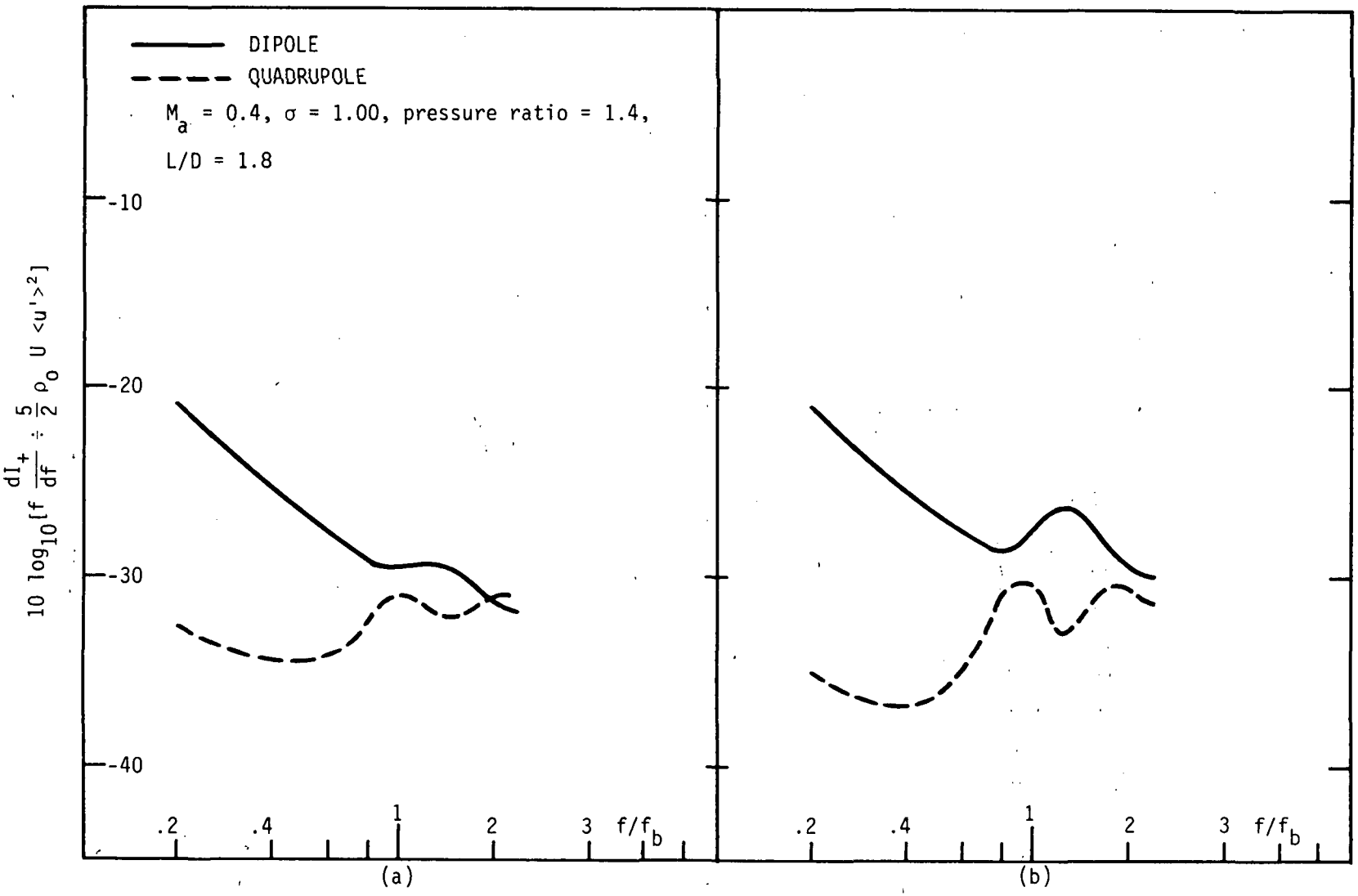

M_t = 0.4

M_t = 0.5, Rest as in 5(a)

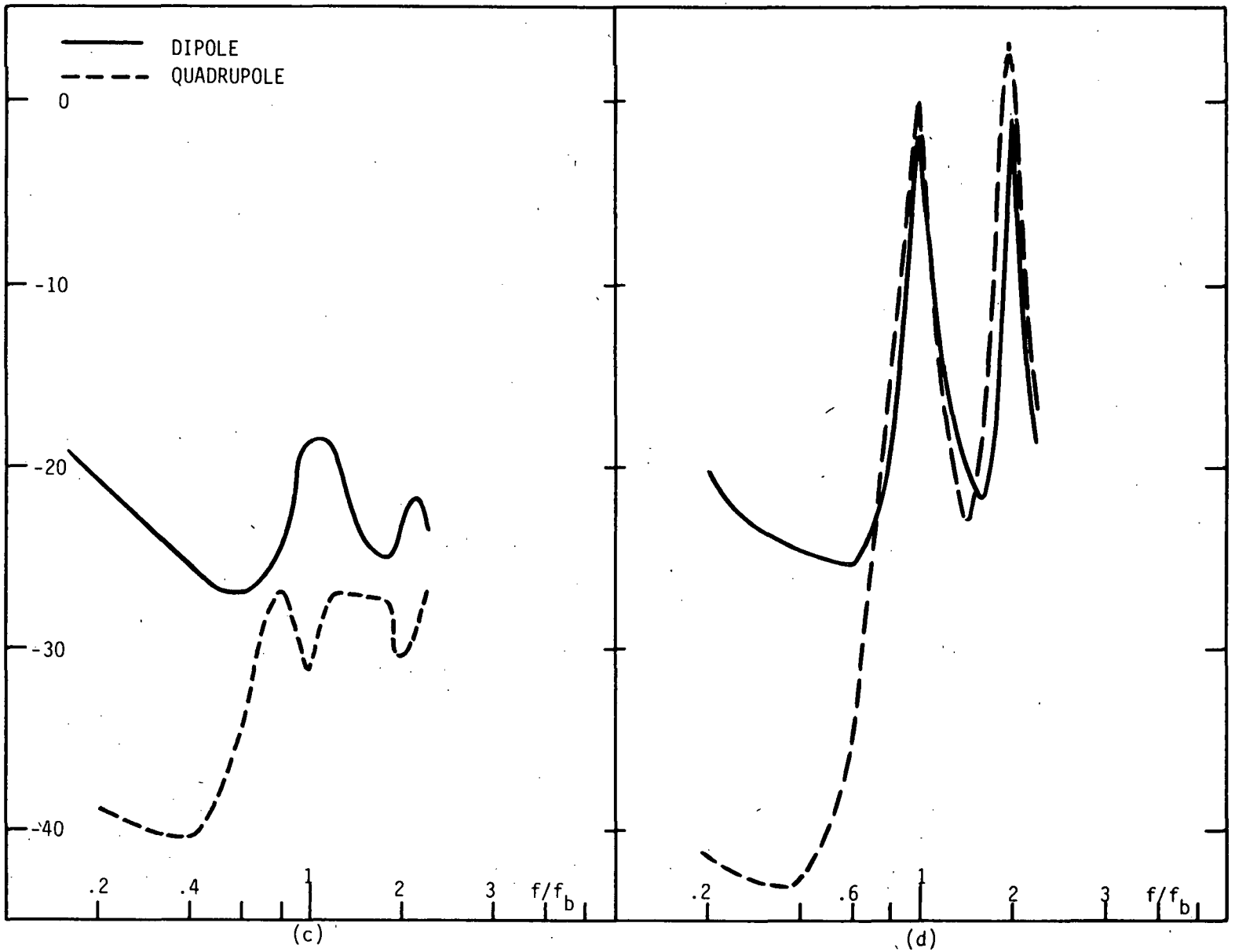

M_t = 0.6, Rest as in 5(a)

M_t = 0.9, Rest as in 5(a)

FIGURE 6. INLET DISTORTION NOISE

FIGURE 7. INLET DISTORTION NOISE

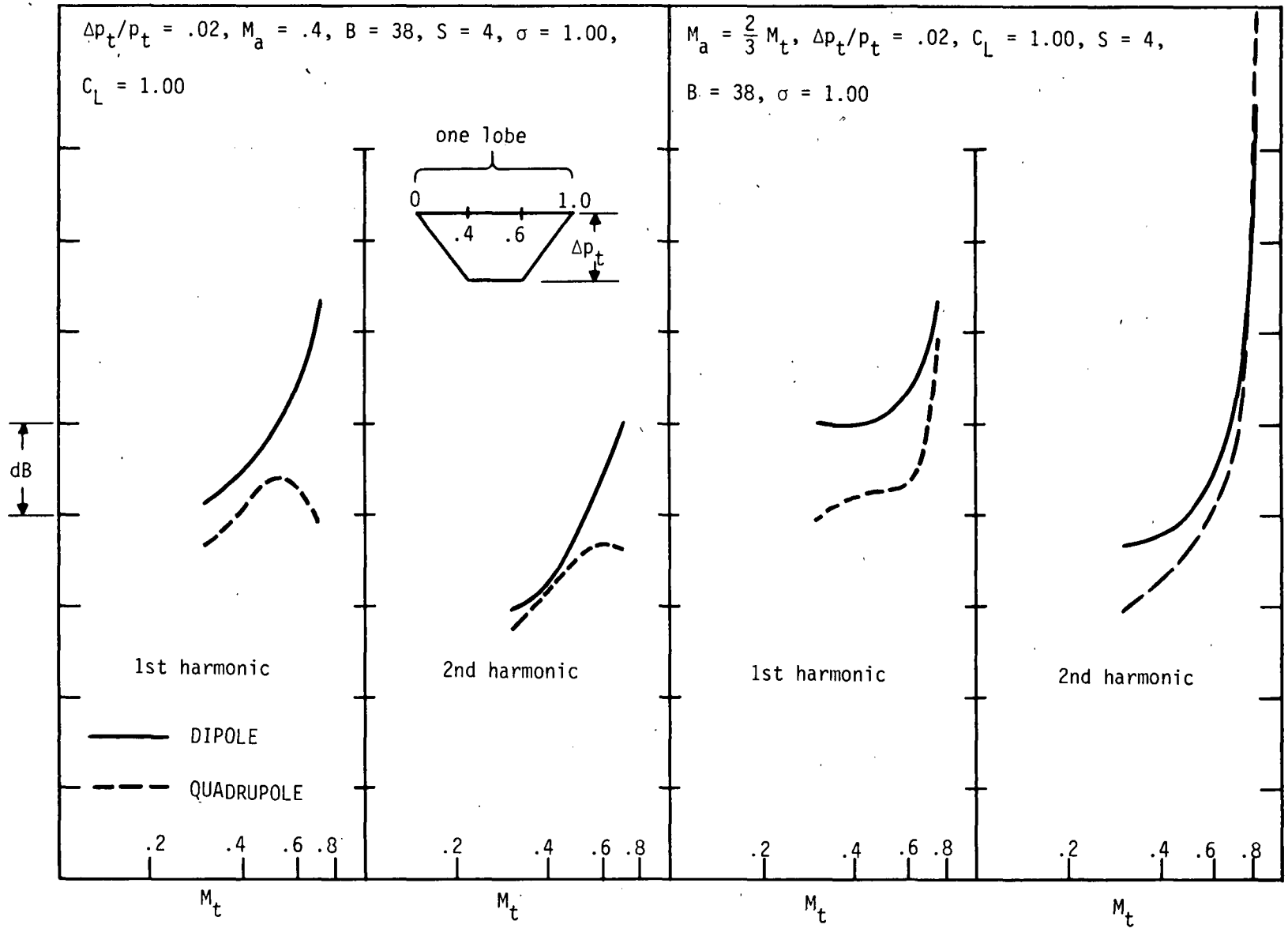

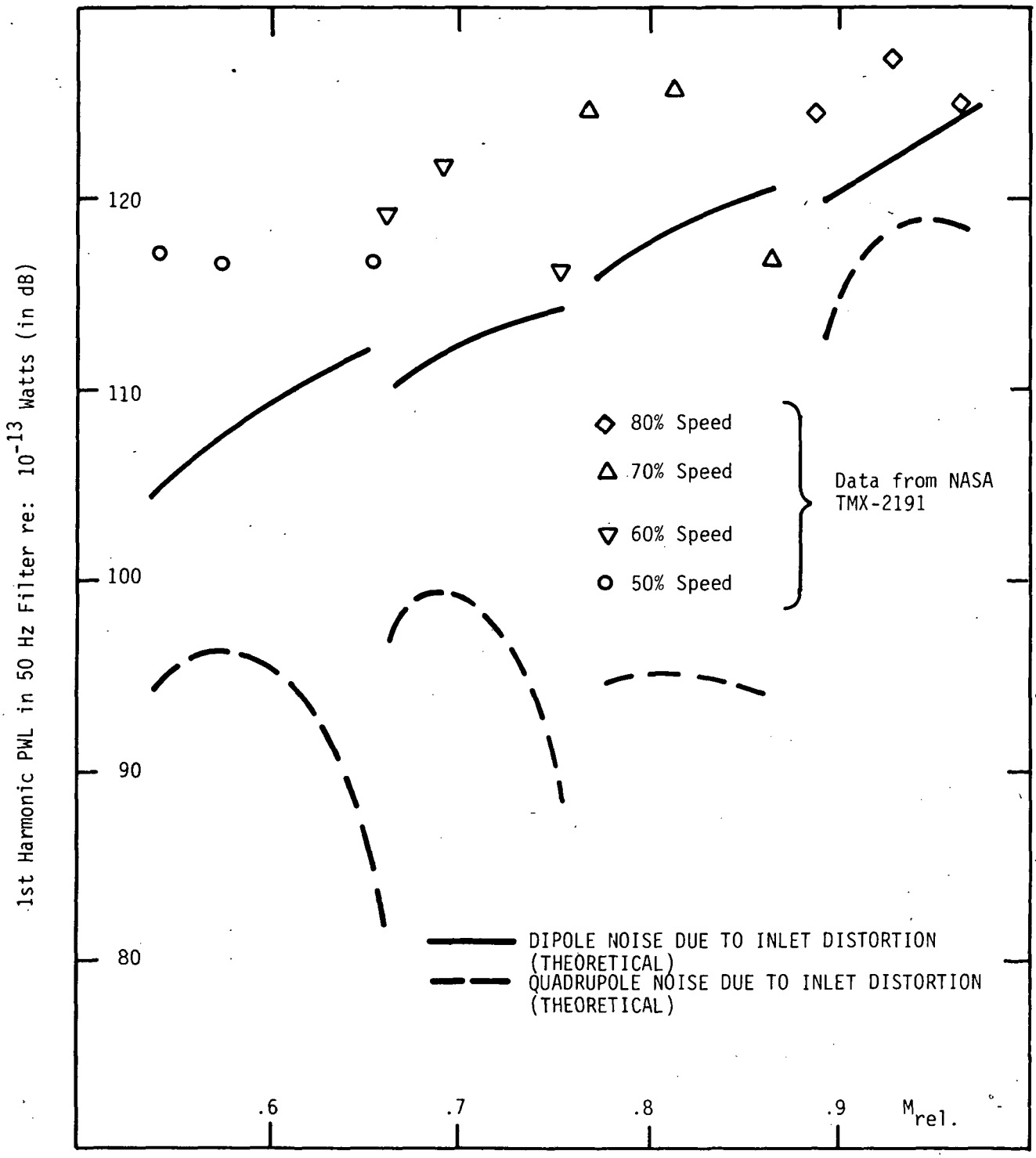

FIGURE 8. COMPARISON WITH (5): ROTOR 1.

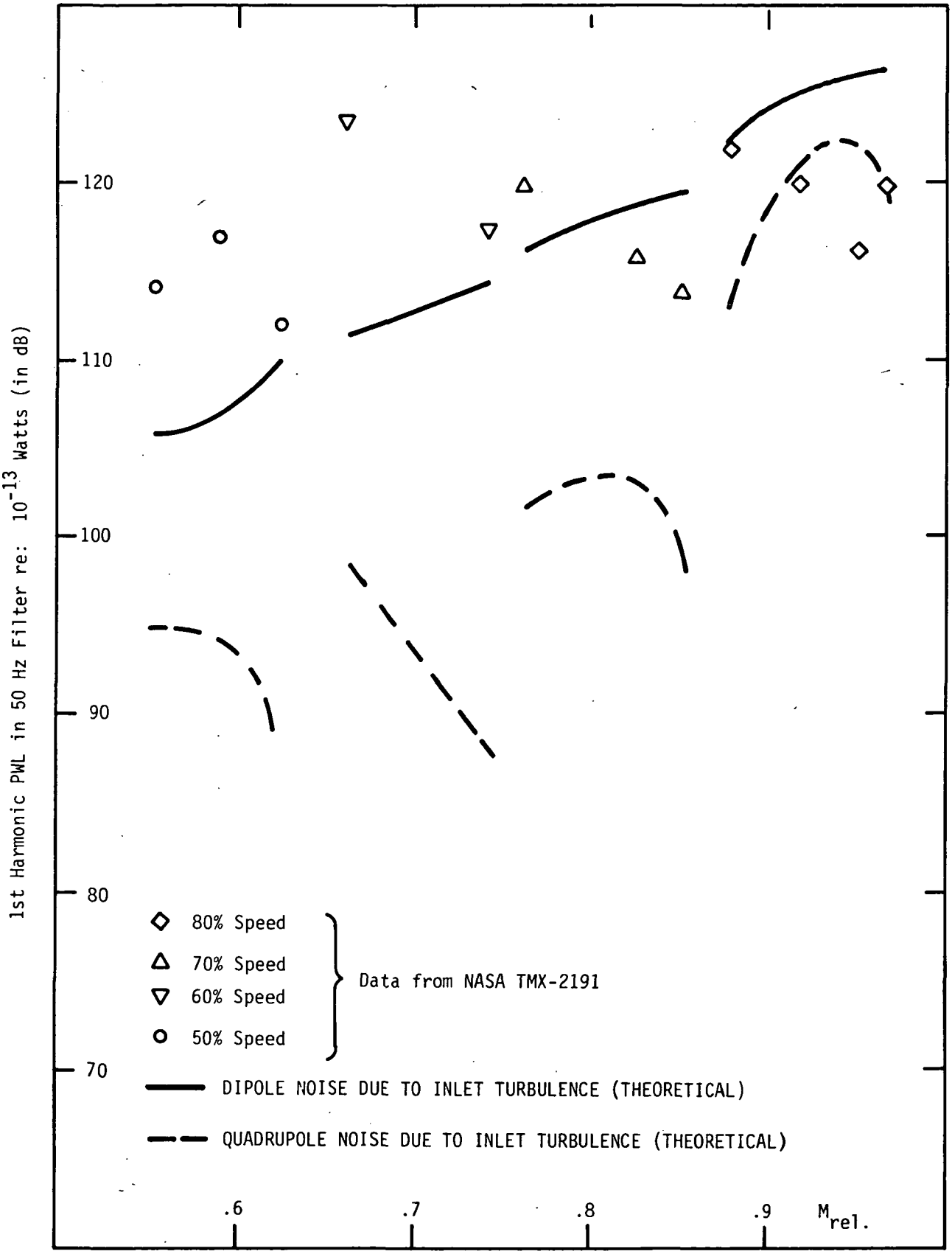

FIGURE 9. COMPARISON WITH (5): ROTOR 2

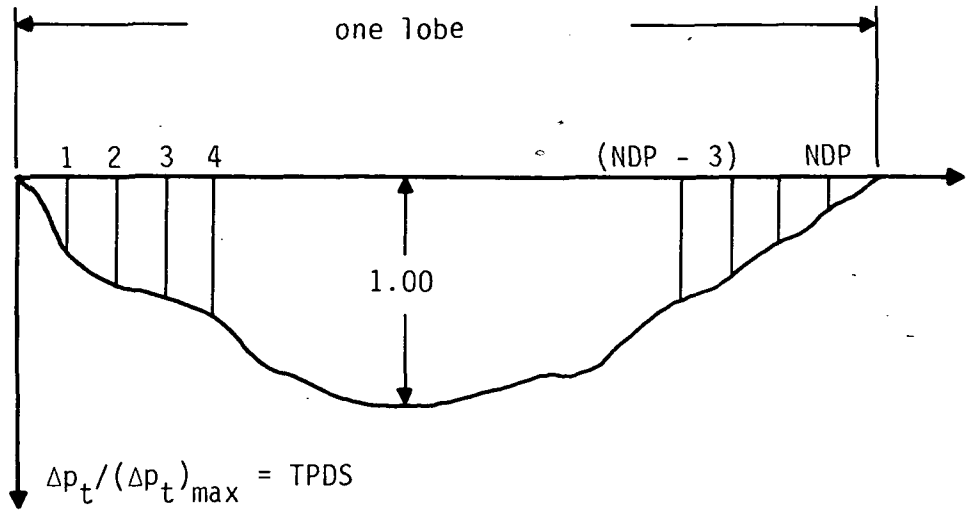

FIGURE A1

DEFINITION SKETCH FOR INPUT FUNCTION TPDS

NASA-Langley, 1974 E-8072

"The aeronautical and space activities of the United States shall be conducted so as to contribute . . . to the expansion of human knowledge of phenomena in the atmosphere and space. The Administration shall provide for the widest practicable and appropriate dissemination of information concerning its activities and the results thereof."

—NATIONAL AERONAUTICS AND SPACE ACT OF 1958

NASA SCIENTIFIC AND TECHNICAL PUBLICATIONS

TECHNICAL REPORTS: Scientific and technical information considered important, complete, and a lasting contribution to existing knowledge.

TECHNICAL NOTES: Information less broad in scope but nevertheless of importance as a contribution to existing knowledge.

TECHNICAL MEMORANDUMS: Information receiving limited distribution because of preliminary data, security classification, or other reasons. Also includes conference proceedings with either limited or unlimited distribution.

CONTRACTOR REPORTS: Scientific and technical information generated under a NASA contract or grant and considered an important contribution to existing knowledge.

TECHNICAL TRANSLATIONS: Information published in a foreign language considered to merit NASA distribution in English.

SPECIAL PUBLICATIONS: Information derived from or of value to NASA activities. Publications include final reports of major projects, monographs, data compilations, handbooks, sourcebooks, and special bibliographies.

TECHNOLOGY UTILIZATION PUBLICATIONS: Information on technology used by NASA that may be of particular interest in commercial and other non-aerospace applications. Publications include Tech Briefs, Technology Utilization Reports and Technology Surveys.

Details on the availability of these publications may be obtained from:

SCIENTIFIC AND TECHNICAL INFORMATION OFFICE

NATIONAL AERONAUTICS AND SPACE ADMINISTRATION

Washington, D.C. 20546